ISSN 0972-0480 • Vol. 27 No. 1 • January 2024

IIM METAL NEWS

A monthly publication of The Indian Institute of Metals

STAR TESTING SYSTEMS

Komputerised Material Testing Systems

Servo Electric [CCG] Single Lever Arm Type

Creep Testing Machine

Series : 9018

SS-4 column type Creep Testing Machines

Series : 9018

Servo-Electric Creep Testing Machines

Creep Testing Machines

Rod - Tube type EXTENSOMETER

With Single LVDT

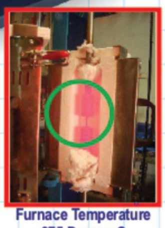

Furnace Temperature 975 Degree C

EXTENSOMER with DIGITAL DIAL GAUGE

Four Rod type EXTENSOMETER

With Dual LVDT

STS offers you **Single Lever Arm Type Creep Testing Machines** for testing in air environment in accordance with **ASTM E-139** testing standards in FOUR ROD column type, Solid C channel type and **Servo - Electric Creep Testing Machine** (with Load Cell) with 3 or 5 Zone High Temperature Furnace (upto 1250 Degree C), Grippers, Adaptors, Creep Compression Test Fixtures, Special Fixtures for Tube Test Adaptors, Dual displacements, measurements systems, one from Cross Head and another from Extensometer, [FOUR ROD Type] or Averaging Extensometer [ROD & Tube type] use full **for testing long duration upto 50,000 Hours**. It comes with high end Data Logging Systems, Computer, Printer with Creep Software Program. Adaptors or Grippers are made from Supper Alloy Materials like Inconel 718, 713 MAR M 246/247 depending on test requirements. Our Machines are available in Capacities of 1000 Kg, 3000 Kg, 5000 Kg, 10,000 Kg and 30,000 Kg [In Newtons equivalent also] Lever Arm Arm is made from solid block. And available in different Lever Arm Ratio like 10 : 1, 20 : 1, and 30 :1.

NOTE : Due to the continuous Research and Developments, Technical Specifications of above all Creep Testing Machines, may change without any notice.

IIM METAL NEWS

Vol. 27 No. 1 January 2024

Chief Editor

Prof K Bhanu Sankara Rao

Printed and Published by
Brig. Arun Ganguli (Retd.) Secretary General, on behalf of "The Indian Institute of Metals", and
printed at Print Max, 44, Biplabi Pulindas Street, Kolkata-700009
and
published at 'Metal House', Plot 13/4, Block AQ, Sector V, Salt Lake, Kolkata-700091, West Bengal, India

E-mail: secretarygeneral.iim@gmail.com
iimmetalnews@yahoo.com
Phone: 033-2367 9768 / 2367 5004
Website: www.iim-india.net
Fax: (033) 2367 5335
Facebook -
https://www.facebook.com TheIndianInstituteofMetals/
Instagram -
https://www.instagram.com/indianinstituteofmetals/
LinkedIn -
https://www.linkedin.com/company/the-indian-institute-of-metals/
Twitter -
https://twitter.com/iimetals_india

Mr. J C Marwah, Former Secretary General, IIM, celebrated his 90th Birthday on 16th December 2023

THE INDIAN INSTITUTE OF METALS

FORMER PRESIDENTS

1946-48	Late J J Ghandy	1977-78	Late V A Altekar	1992-93	Late A C Wadhawan	2007-08	Late Srikumar Banerjee
1948-50	Late P Ginwala	1978-79	Late T R Anantharaman	1993-94	Late R Krishnan	2008-09	Mr L Pugazhenthy
1950-52	Late Phiroz Kutar	1979-80	Late P L Agrawal	1994-95	Dr S K Gupta	2009-10	Dr Sanak Mishra
1952-54	Late G C Mitter	1980-81	Late EG Ramachandran	1995-96	Mr R N Parbat	2010-11	Dr D Banerjee
1954-56	Late M S Thacker	1981-82	Late C V Sundaram	1996-97	Late P Rodriguez	2011-12	Mr M Narayana Rao
1956-58	Late K S Krishnan	1982-83	Late Samarpungavan	1997-98	Late S Das Gupta	2012-13	Mr H M Nerurkar
1958-60	Late S K Nanavati	1983-84	Late J Marwaha	1998-99	Dr C G K Nair	2013-14	Prof K Chattopadhyay
1960-62	Late G K Ogale	1984-85	Late A K Seal	1999-00	Prof S Ranganathan	2014-15	Dr R N Patra
1962-65	Late Dara P Antia	1985-86	Late J J Irani	2000-01	Mr V Gujral	2015-16	Mr S S Mohanty
1965-67	Late B R Nijhawan	1986-87	Late Y M Mehta	2001-02	Late P Parvathisem	2016-17	Prof Indranil Manna
1967-70	Late M N Dastur	1987-88	Late V S Arunachalam	2002-03	Late P Ramachandra Rao	2017-18	Dr Biswajit Basu
1970-72	Late Brahm Prakash	1988-89	Late S R Jain	2003-04	Late S K Bhattacharyya	2018-19	Mr Anand Sen
1972-74	Late P Anant	1989-90	Late L R Vaidyanath	2004-05	Dr T K Mukherjee	2019-20	Dr U Kamachi Mudali
1974-76	Late FAA Jasdanwalla	1990-91	Dr P Rama Rao	2005-06	Late Baldev Raj	2020-21	Prof Amol A Gokhale
1976-77	Late S Visvanathan	1991-92	Dr T Mukherjee	2006-07	Mr B Muthuraman	2021-22	Mr T V Narendran
						2022-23	Dr Samir V Kamat

FORMER SECRETARIES / SECRETARY GENERALS*

1946-57	Late Dara P Antia	1977-86	Late L R Vaidyanath	1997-06	Mr J C Marwah	2013-15	*Mr Bhaskar Roy
1958-67	Mr R D Lalkaka	1986-97	Late S S Das Gupta	2006-13	*Mr J C Marwah	2015-18	*Mr Sadhan Kumar Roy
1968-76	Dr M N Parthasarathi					2018-23	*Mr Kushal Saha

Dr Daya Swarup Memorial Lecture 2023

Multicomponent High Entropy Alloys : A Renaissance in Physical Metallurgy

N K Mukhopadhyay

Department of Metallurgical Engineering,
Indian Institute of Technology (Banaras Hindu University)
Varanasi 221 005
Email: mukho.met@iitbhu.ac.in

Introduction

I feel highly privileged and honored for being selected for delivering the 'Dr. Daya Swarup Memorial Lecture 2023' of the Indian Institute of Metals (IIM). I would like to express my sincere thanks to the IIM Council and the Award Committee for inviting me to deliver this lecture. Prof. Daya Swarup was the doyen of Metallurgical Education in India. I consider myself fortunate to be associated as a faculty member with the same Department where Dr. Daya Swarup (1904-1983) was an alumnus (1928) and a teacher. In fact, he was among the second batch of students completing undergraduate degree, B.Sc (Met. Engg.) in the Department under the Headship of Prof N.P. Gandhi. He served as a Professor and Head of Department (1937-1962), and Principal of the erstwhile College of Mining and Metallurgy (1944-62) of the Banaras Hindu University, Varanasi. He was responsible for the emergence of the Department as a postgraduate institution. During his tenure, the MSc (Met. Engg.) course was started in 1957 and the first ever Ph.D. (Met Engg.) degree in India was awarded in 1955. His efforts had acted as the guiding spirit for the Institute and paved the way to what it is today, Department of Metallurgical Engineering, Indian Institute of Technology (Banaras Hindu University), Varanasi. Now, it is important to point out that the Department is observing the Centenary Celebration throughout the Year 2023. His books on metallurgy motivated and inspired metallurgists of that era all over India. In commemoration of Dr. Daya Swarup's seminal contributions to metallurgical education in India, in this presentation, I would like to share some of our interesting work related to the 'High Entropy Alloys', which have aroused a tremendous excitation among the Physical Metallurgists, Materials Scientists and Engineers to explore the various facets of this class of novel materials.

High Entropy Alloys (HEAs)

It is known that Physical Metallurgy deals with various issues of metallic alloys pertaining to the composition and processing routes leading to evolution of different phases having a variety of structures and microstructures and the resultant properties aimed at designing and developing metallic alloys useful for technological applications. In 1926, the rules for the formation of a binary solid solution of metallic elements in a crystalline framework, which was considered as one of the important steps for successful alloy design, were proposed by William Hume-Rothery considering the atomic size, electronegativity, valence electrons and crystal structure of the individual metallic elements. Intermetallics or composites of immiscible elements are expected to form if the Hume-Rothery rules for solid solution formation are not satisfied. However, after the discovery of concentrated multicomponent solid solution alloys, there was a need to understand the principles underlying the formation of solid solutions containing five or more elements in high concentration. J. W. Yeh (Taiwan) first suggested that the stability of the solid solutions could be attributed to the high entropy arising due to randomness in the configuration of atoms in solid solutions. Thus, the concept of high entropy alloy (HEA) was advocated by him [1] in 2004, while interpreting the stabilization of these multicomponent equiatomic or near-equiatomic disordered solid solutions in metallic alloys. It is pertinent to point out that Brian Cantor (UK) independently worked on multicomponent alloys similar to HEAs since 1980 [2].The multimetallic combination of metals was termed as 'multimetallic cocktails' by S. Ranganathan [3] in 2003 and became the first journal publication heralding this new field of alloys. Now, for multicomponent concentrated alloys the formal definition of this special class of materials (HEAs) has been put forward as an alloy containing five or more elements with concentration ranging from 5% to 35% (at%), leading to a simple disordered solid solution structure. Interesting aspects of the work reported on HEAs are reviewed early in the book by Murty et al. [4].

It is a matter of pride for us that this first book on the new realm of research is authored by two Indians and a Taiwanese. There is now a lot of excitement and new activities, as it has opened up several fronts for discovering newer alloy systems for demanding technologies. In a way it has ushered in *'A Renaissance in Physical Metallurgy'* [5]. Keeping in view the current excitement and interesting activities in this area, there are several thousands of published papers, many patents and also international workshops and conferences organized all over the globe. Earlier, S. Ranganathan [3] highlighted the multicomponent alloys in the context of bulk metallic glasses and HEAs. He emphasized the importance of cocktail effects in multimetallic alloys. He attributed cocktail effects in the multicomponent system to the extension of solid solution. In the literature reports on HEAs ranging from theoretical modeling and simulation, thermodynamics, synthesis, processing, characterization, property evaluation and possible applications. However, in addition to high entropy three other core effects such as sluggish diffusion, lattice distortion and cocktail effects were also proposed. Figure 1 discerns the variation of configurational entropy with respect to number of alloying elements in equiatomic high entropy elements. It was observed that on increasing number of alloying elements in HEAs, the configurational entropy initially increases and then become almost stagnant.

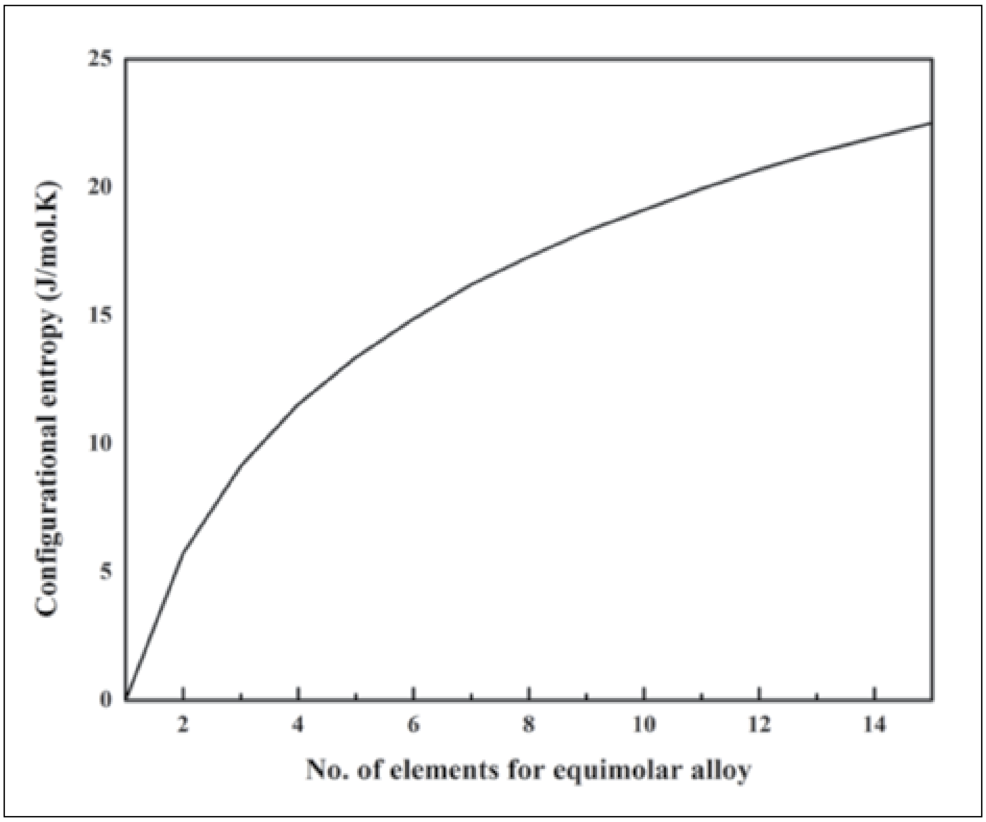

Fig. 1 : The variation of configurational entropy ($\triangle S_{conf}$) for an equimolar alloy with a number of elements.

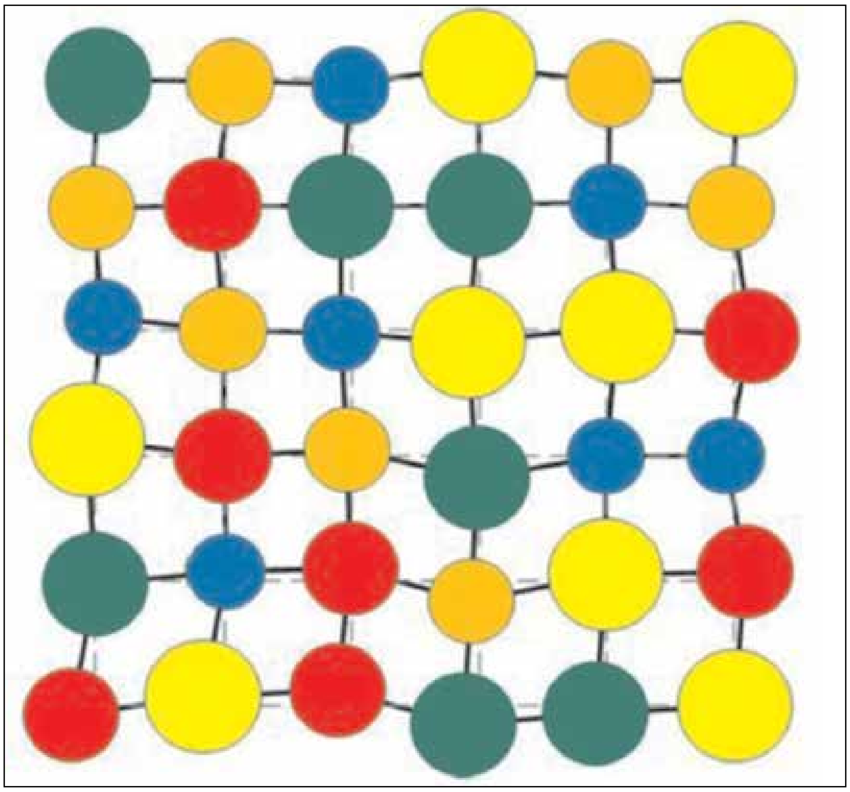

Fig. 2 : The schematic representation of strained lattices in HEAs [6].

Due to various sizes of atoms in the multicomponent alloys, lattice is anticipated to highly strained and the schematic diagrams suggests typical strained lattices in HEAs [Figure 2]. Hence, the fundamental deformation science should be addressed differently in the context of HEAs unlike conventional alloys, involving three distinct factors encompassing strain rate dependence, role of nanotwinning and grain size dependence. It has been emphasized that the formation of nanocrystalline HEAs has made them more interesting due to their fundamental and technological importance [7–9]. It has been elaborated the possible application (among various other applications) of HEAs should be explored in three niche areas – advanced ultra super critical (AUSC) coal-powered station, radiation environment, and aero-gas turbine engines [10,11]. Evaluating the data, it is suggested that for AUSCs the following components can be investigated: (i) oxide dispersion strengthened low stacking fault energy FCC alloys such as Cantor alloy i.e., CrMnFeCoNi with Y_2O_3 dispersions; (ii) high-strength $AlCrFeCoNi_2$ alloy with minor additions of Mo, Ti, or Si, either singly or in combination and (iii) FCC HEA matrix with B2 dispersions such as $AlCoNiFeTi_{0.4}$ and $Al_{0.3}CrFeCoNi$. For radiation environment with reference to fast breeder reactor fuel clad a combination of AlSiTiCrFeMo, not necessarily in equal atomic proportions, such that it leads to a low SFE BCC alloy with adequate ductility and strength to be explored. For high-pressure gas turbine rotors, a multiphase HEA from AlTiCrFeNiNbMo as well as VTaMoNbW may be worth considering.

Low-density high entropy alloys (LDHEAs)

In recent times thrust for development of low-density high entropy alloys (LDHEAs) have gained impetuous for meeting the requirements of modern-day industry. Among the various classes of LDHEAs, the HEAs containing low-density elements like Mg, Al, Li, Ti, Be, Sc, Si etc. have gained some attention in recent times by the scientific community. A few researchers and co-workers have made significant efforts in understanding the microstructure and mechanical properties of LDHEAs containing elements like Sc, Be, Mg, Ti etc. The work of Vinod kumar and co-workers on LDHEAs needs special mention [12]. They have discerned the influence of elemental composition on the phase evolution, thermal stability and mechanical properties of $Mg_xAlCrFeCu$ (x = 0, 0.5, 1.0, 1.7 at%) LDHEAs prepared by milling and spark plasma sintering (SPS). The MA of AlCrFeCu and $Mg_{0.5}AlCrFeCu$ LDHEA for 20 h has led to the formation of a two-phase structure of BCC (major) and FCC (minor). Moreover, it has been observed that the lattice parameter of FCC is close to Cu. On increasing the amount of Mg in $Mg_xAlCrFeCu$ (x = 1.0, 1.7) LDHEA, two BCC phases were formed [12]. However, a more cost-effective alloy design strategy needs to be adopted for design and development of LDHEAs.

In the present lecture, I will be briefly discussing some of our recent work on MgAlSiCrFe, MgAlSiCrFeNi, MgAlSiCrFeCuZn, MgAlMnFeCu LDHEAs[13–16]. These LDHEAs were having experimental density in the range of 4 to 5.5g.cm^{-3}. These LDHEAs were prepared by mechanical alloying followed by spark plasma sintering (SPS) at 800^{0}C. The alloying behavior, phase evolution, phase composition, and thermal stability of as-milled nanostructured LDHEAs powders were determined by X-ray diffraction techniques, transmission electron microscopy, scanning electron microscopy, and differential scanning calorimetry (DSC). The milling of elemental powders of MgAlSiCrFe for 60 h led to the formation of HEA having BCC phase with a lattice parameter of 0.2887 ± 0.005 nm (close to that of the α-Fe) along with minor fraction of undissolved Si (Figure 3).

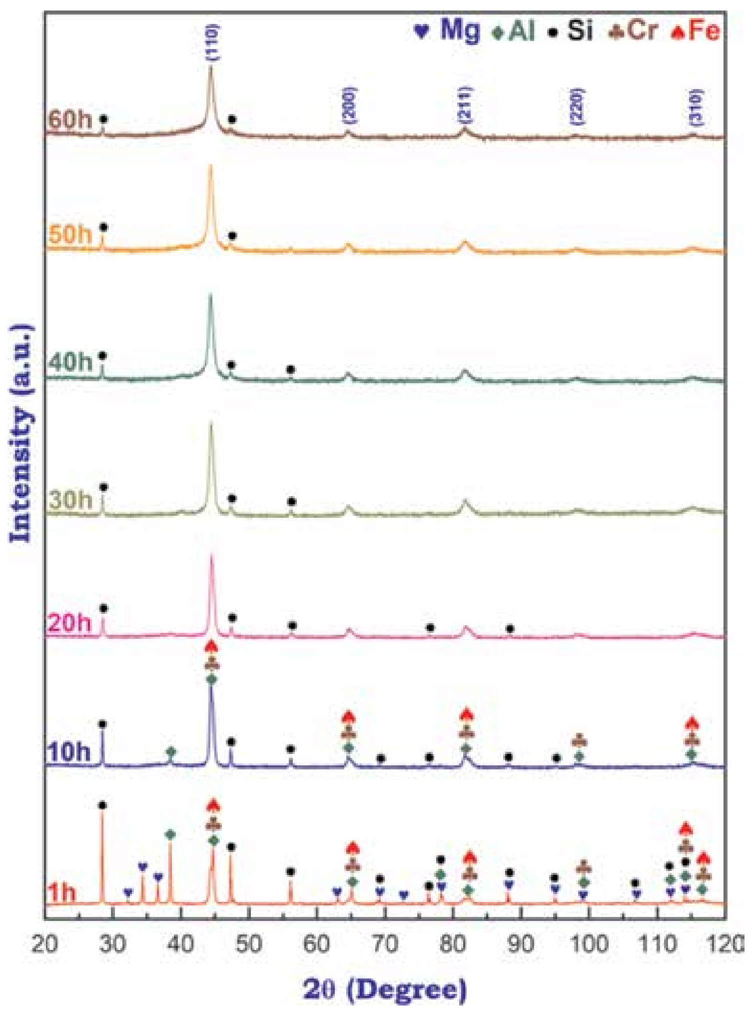

Fig. 3 : Phase evolution during mechanical alloying of MgAlSiCrFe high-entropy alloy milled up to 60 h [13].

The nanostructured HEA powders having crystallite size and grain size of ~19 nm was formed after milling. The STEM–EDS mapping of these milled powders confirms uniform elemental distribution following 60 h of MA (Figure 4). The DSC thermogram of 60 h milled HEA powder demonstrates the powder's thermal stability up to 400 ^{0}C. The exothermic heating events detected in the DSC thermogram correspond to phase transformation of MgAlSiCrFe HEA powder and may be corroborated with the phases observed in ex-situ XRD analysis of HEA powders annealed at various temperatures up to 700^{0}C. The systematic investigation discerns the presence of parent BCC phase along with other minor phases i.e. B2 type Al–Fe phase, FCC phases (Al–Mg solid solution), Cr_5Si_3, Mg_2Si, and $Al_{13}Fe_4$. Additionally, this work correlates the experimental results with a variety of thermodynamic parameters in order to understand the phase evolution and stability. This work also showed the phase evolution, chemical composition, and microstructure of the SPSed sample consolidated at 800^{0}C (1073 K) through XRD and SEM techniques. The SPSed samples exhibited the formation of B2-type AlFe phase (a=0.2889 nm) along with the parent disordered BCC phase and minor fraction of $Al_{13}Fe_4$, β-Al_3Mg_2, and Cr_5Si_3. The instrumented micro-indentation technique was used to examine the mechanical properties of the LDHEA. The hardness and yield strength were found to be approximately 7.0 GPa and 2.1 GPa with an appreciable relative density of 99.98% for the SPSed sample.

The equiatomic MgAlSiCrFeNi LDHEA milled powder shows the formation of a BCC phase having lattice parameter of 0.2876±0.03 nm and undissolved Si (~3 at%) after 60 h of milling. The structural evolution and fine microstructural characteristics were examined under TEM (Figure 5). The micrographs showing bright field images (a, d) and selected area diffraction patterns (SADPs) (b, e), and dark field images (c, f) of 60 h MM powder

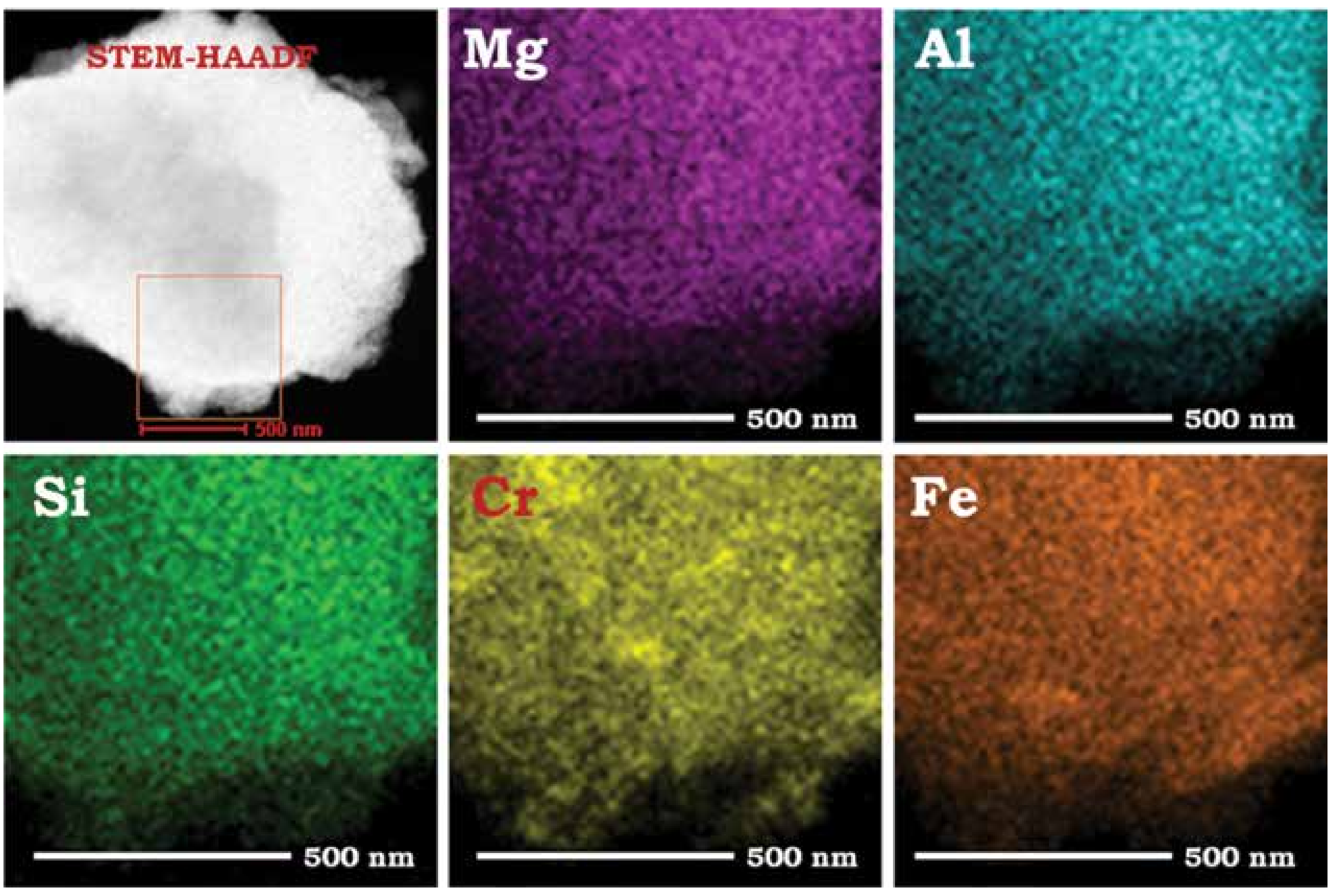

Fig. 4 : STEM–EDS mapping of equiatomic MgAlSiCrFe high-entropy alloy mechanically alloyed for 60 h showing homogenous elemental distribution[13].

reveals the presence of a BCC phase coexisting with the minor amount of undissolved Si. The bright-field image (Figure 5 (a)) reveals the heavy deformation induced during the MA and can be observed in the powder particle. The grains of ≤20 nm were also identified in the milled powder particles. These observations agree well with the results of XRD experiment of 60 h MM powder revealing considerable peak broadening. Figure 5(b), reveal the polycrystalline nature of the alloy by forming the ring pattern corresponding to the BCC phase. These rings are indexed as (110), (200), and (211) planes of BCC phase. Figure 5 (c) shows dark field image collected from the (110) plane, which confirms the nanocrystalline nature of the milled powder of sizes ~15 ± 4 nm.

The DSC experiment up to 1200^{0}C (1473 K) shows five exothermic heating events (Figure 6) corresponding to various phase transformations, which were co-related with the results obtained from ex-situ XRD analysis of annealed powder at elevated temperatures (Figure 7). The phase transformation events during annealing at different temperature up to 800^{0}C (1073 K) resulting in the formation of a major B2 type phase (a=0.289 nm) and BCC phase along with small amounts of FCC Al-Mg solid solution phase (FCC 1 (a=0.4082 nm) and FCC 2 (a=0.4215 nm)), monoclinic $Al_{13}Fe_4$ (a=1.549 nm, b=0.808 nm, c=1.248 nm, α=β=90°), Mg_2Si (a=0.6351 nm), Cr_5Si_3 (a=b=0.9165nm, c=0.4638 nm). The SPSed sample also exhibits BCC and B2-type phases coexisting with minor amounts of other phases observed for 800^{0}C (1073 K) annealed sample. In this work, it has been observed that the co-existence of minor phases with parent BCC phase in SPSed alloy (having relative density of ~99.40%) has led to significantly high hardness and modulus of elasticity of ~9.98±0.3 GPa and 229±0.3 GPa respectively.

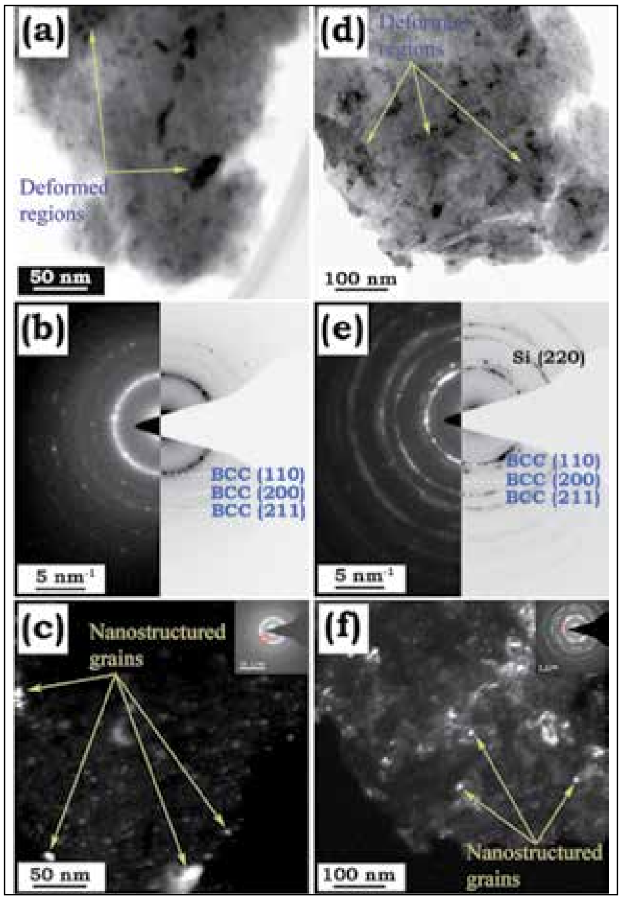

Fig. 5 : TEM micrographs showing (a, d) bright field images and (b, e) selected area diffraction patterns and (c, f) dark field images of LDHEA powder milled after 60 h MM showing presence of BCC along with minor fraction of Si [15].

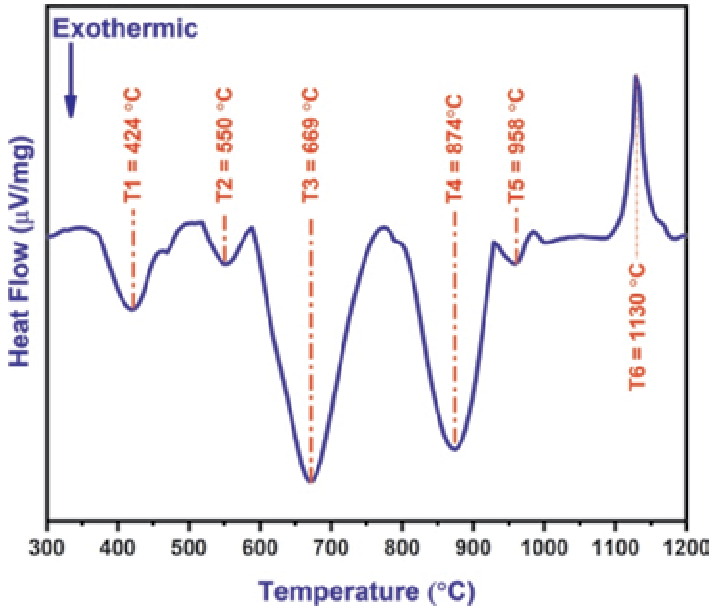

Fig. 6 : DSC thermogram of MgAlSiCrFeNi powder milled for 60 h exhibiting exothermic and endothermic events [15].

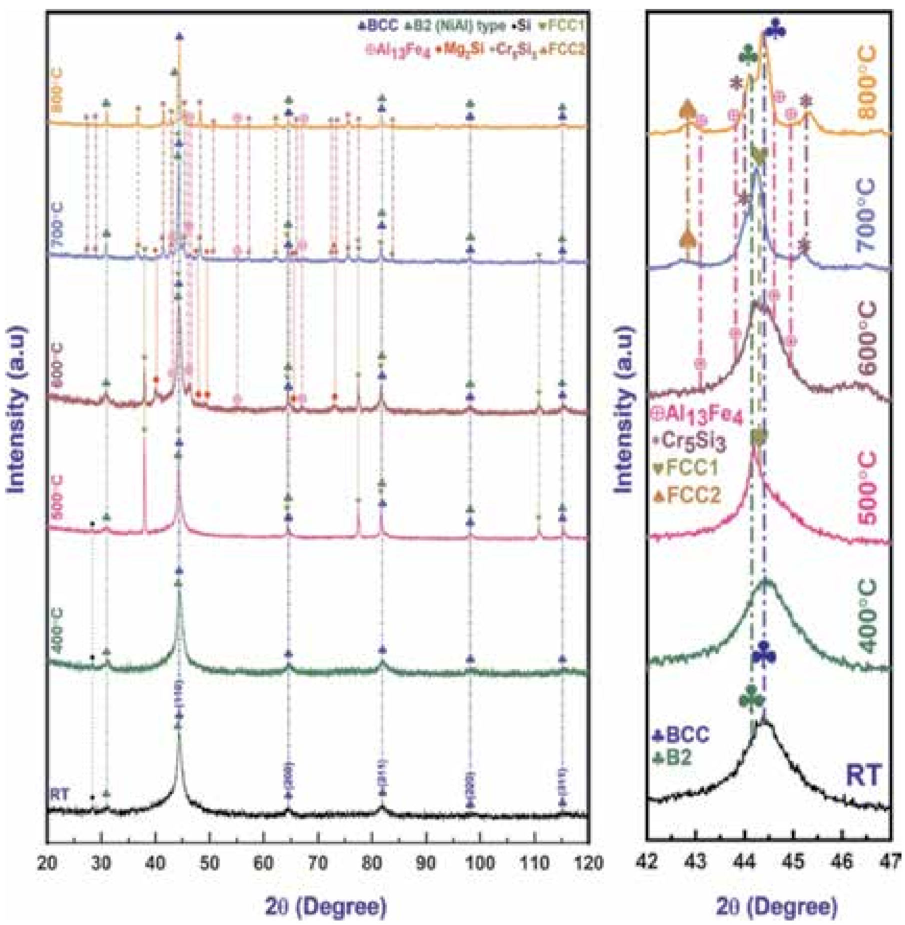

Fig. 7 : (a) Phase formation during annealing of 60 h milled MgAlSiCrFe HEA powder upto 800 °C (1073 K); (b) magnified image for (110) peak of the BCC phase for revealing evolution of other phases [15].

In continuation to the previous quaternary and hexanary LDHEAs, efforts were made to investigate the structure, microstructure and mechanical properties of equiatomic septenary MgAlSiCrFeCuZn high entropy alloy synthesized by mechanical alloying for 60 h followed by spark plasma sintering. The mechanical alloying led to the formation of major BCC phase (having lattice parameter of 0.2895 nm) with minor fraction of retained Si. The thermal stability of the milled powders was discerned through DSC thermogram up to 1200^{0}C (1473 K) and the various exothermic heating events observed were corroborated with the phases observed in the ex-situ XRD of annealed powders. The MgAlSiCrFeCuZn HEA was consolidated at 800^{0}C using SPS. The hardness and yield strength of SPSed samples were determined using instrumented instrumentation techniques. It was observed that for the conventionally sintered sample the hardness was ~6.0 GPa, however for the SPSed sample it was found to be ~9.0 GPa. The excellent indentation hardness may be due to the appreciable density of the SPSed sample.

Further, efforts were also made to synthesize and characterize low-density MgAlMnFeCu HEA. The low-density MgAlMnFeCu HEA has been synthesized by mechanical alloying (MA). Milling up to 60 h leads to the formation of a mixture of two phases consisting of a BCC phase (a = 2.87 ± 0.02 Å) and γ-brass type phase (a = 8.92 ± 0.03 Å), with ~2 μm powder particle size. The as-milled alloy after spark plasma sintering (SPS) at 900 ˚C exhibits an experimental density of 4.946 ± 0.13 g cc-1, which is 99.80% of the theoretical density. SPS leads to the formation of C15 Laves phase ($MgCu_2$ type; a = 7.034 ± 0.02 Å) and B2 (AlFe type; (a = 2.89 ± 0.02 Å) intermetallics along with the γ-brass type phase. The SPSed sample has exceptional hardness value (~5.06 GPa), high compressive strength (~1612 MPa) and appreciable failure strain (~6.4%) coupled with relatively low density.

The present work also focuses on calculating thermodynamic parameters, in order to correlate the experimental findings of phase evolution and stability of the annealed powder and spark plasma sintered quaternary, hexanary and septenary LDHEAs. The work also describes the phase evolution during MA and SPS using Thermo-Calc software with the help of property diagrams, which were generated through the CALPHAD approach. The phases observed experimentally and through property diagrams were not exactly correlated to each other. The main reason for this anomaly may be attributed to the absence of TCHEA database for HEAs containing low-density elements like Mg, Sc, Be etc.

High entropy steels

The surge for development of near or non-equiatomic high entropy alloys has led to conceptualization of high entropy steels (HES). This idea of HES was initially mooted by the Raabe and co-workers at MPIE, Germany in 2015 [17]. Most of the initial reports on HES have employed liquid metallurgical processing of fabrication of these materials. However, these routes often result in coarse microstructure accompanied with other issue pertaining to segregation, porosity etc. Here we will give an overview on the recent development of a few non-equiatomic $Fe_{40}Mn_{19}Ni_{15}Al_{15}Si_{10}C_1$ (at. %) [18]), $Fe_{40}Mn_{14}Ni_{10}Cr_{10}Al_{15}Si_{10}C_1$ (at. %) [19], $Fe_{40}Mn_{14}Ni_{10}Ti_{10}Al_{15}Si_{10}C_1$ (at. %) [20] high entropy steels prepared by mechanical alloying followed by spark plasma sintering. The $Fe_{40}Mn_{19}Ni_{15}Al_{15}Si_{10}C_1$ (at. %) high entropy steel milled for 35 h results in the formation of multiphase structures i.e., a major BCC phase (a = 0.286 nm; cI2) along with minor fraction corresponding to γ-brass type (a = 0.872 nm; cI52) and ordered B2-type (a= 0.290 nm; cP2) phases with the trace amount of retained Si as shown in the Figure 8.

The milled powder was found to be thermally stable up to ~500^{0}C, however, the formation of Fe_5Si_3-type silicide phase was evident at ~520 °C. The spark plasma sintered (SPSed) sample was able to retain the BCC phase, B2 and γ-brass type along with the formation of Fe5Si3 type silicide phase (a = b = 0.667 nm, c = 0.468 nm; hP16). These SPSed HES sample was found to have low density (~6.49 ± 0.3 g cm^{-3}), high microhardness (~7.8 ± 0.3 GPa) and good compressive strength (~2046 ± 160 MPa) with an appreciable ductility of ~19% (Figure 9).

The enhanced mechanical properties of the SPSed sample can be attributed to dual-phase microstructure i.e., BCC and B2 along with finer nano-sized silicide precipitates leading to dominant

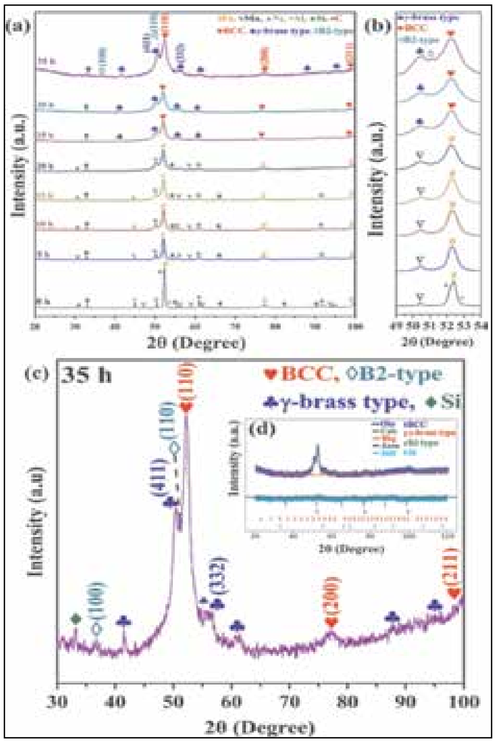

Fig. 8 : (a) XRD patterns of the milled samples at various milling time; (b) Enlarged view in the range of 2θ (degree) = 49°-54°; (c) XRD pattern of the 35-h milled sample; (d) Rietveld refinement of the corresponding 35 h milled sample. This shows the alloying behavior of alloy as a function of milling time, and formation of the multi-phase structure (ferrite as a major phase) after 35 h of milling [18].

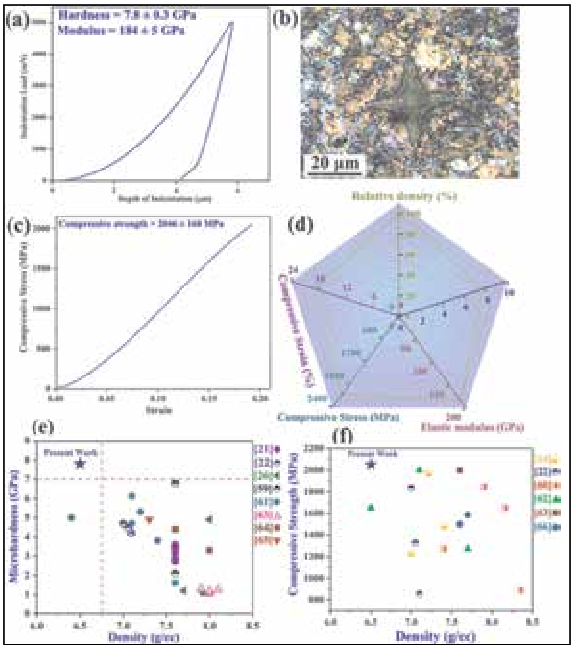

Fig. 9 : (a) Depth of penetration vs Indentation load (p-h plot); (b) Optical micrograph of the indent on SPSed HES sample; (c) Compressive engineering stress and strain curve; (d) Radar diagram showing comparison of different mechanical properties; (e and f) Comparison (microhardness vs density, and ultimate compressive stress vs density) of the present work with the conventional steel and other HEAs. This illustrate the physical and mechanical properties of the SPSed pellet [18].

strengthening mechanisms (i.e., grain-boundary and dislocation strengthening). Further, these HES has shown better wear resistance and biocompatibility in contrast to 316 L stainless steel. The specific wear rate of these HES was found to be ~1.79 × 10^{-5} mm^3/mN and better biocompatibility as compared with 316 L.

In contrast to the previous work, the 40 h milling of $Fe_{40}Mn_{14}Ni_{10}Cr_{10}Al_{15}Si_{10}C_1$ high entropy steel led to the formation of a major BCC phase (a = 0.286 nm) and χ-type phase (close to gamma brass structure). The milled powder sample showed the thermal stability up to 400°C, then showed phase transformation at elevated temperatures. The FCC (a = 0.362 nm) and B2 (a = 0.290 nm) phases, along with Cr_3Si (a = 0.455 nm) and $Cr_{23}C_6$ (a =1.062 nm) precipitates formed after spark plasma sintering. The SPSed sample showed density of 6.8 g.cm^{-3}. These SPSed HES also show excellent hardness (~7.4 GPa), good compressive strength (1962 MPa) and better wear properties (~0.99 × 10^{-5} $mm^3.m^{-1}N^{-1}$). Further this alloy exhibits better biocompatibility as compared to 316 L.

Similarly, efforts were made to understand the phase evolution, microstructure, thermal stability, mechanical and wear properties, and biocompatibility of the $Fe_{40}Mn_{14}Ni_{10}Ti_{10}Al_{15}Si_{10}C_1$ (at. %) high entropy steel. The 30-h milled powder was found to have a dual-phase containing a major BCC (a = 0.287 nm; cI2) and a γ-brass type (a = 0.889 nm; cI52) phase having nanostructured grains of ~10 ± 2 nm. The differential scanning calorimetry (DSC) thermogram exhibited the four exothermic heating events at 530°C, 690°C, 860°C and 1000°C. The phase transformation corresponding to the heating events was correlated with the ex-situ XRD of the as-milled powder. The SPSed HES were found to have a dual-phase structure containing a major FCC phase (a= 0.362 nm; cF4) and a minor BCC phase along with the intermetallic phases like Fe_5Si_3 type (a = b = 0.678 nm, c = 0.475 nm; hP16) and TiC (a = 0.431 nm; cF8). The mechanical properties of these SPSed samples were discerned through instrumented microhardness and compression tests. The microhardness, elastic modulus, ultimate compressive strength and strain were found to be ~10.4 GPa, ~209 GPa, ~2305 MPa and ~15% respectively. This SPSed HES showed an excellent room temperature microhardness and strength which can be attributed to the co-existence of FCC phase along with the minor BCC phase and hard intermetallics. The strengthening mechanism suggested that the grain boundary, dislocation, and precipitates strengthening were dominant. Further, wear and biocompatibility behaviour of the SPSed samples were done, and the specific wear rate is found to be 1.62 × 10^{-5} mm^3/mN and better biocompatibility as compared with 316 L. These HES materials can be exploited for biomedical applications due to its excellent mechanical properties and biocompatilbity.

In view of the existing structure, microstructure, mechanical properties and biocompatibility exhibited by HES, further efforts were made to explore a few non-equiatomic Fe-based HEAs. These Fe-based HEAs having a nominal composition of $Fe_{40}Mn_{20}Cr_{20}$-xNix$Ti_{10}Al_{10}$ (*x = 0, 5, 10* at. %) HEAs were prepared by 40 h of MA followed by SPS. The 40-h milled Fe-based HEAs were found to have a major along with minor fraction corresponding to χ-type phase. The milled powder of Fe-based HEAs have discerned thermal stability up to 500°C, and then formed FCC solid solution in all the three-alloy system. The BCC (major) phase transformed to dual phase i.e., FCC + BCC and further to FCC (major) phase as the Ni content increases from x = 0, 5, and 10 at. % after spark plasma sintering. The microhardness and yield strength values of the SPSed sample decreased from 6.4 GPa to 4.2 GPa, and 1961 MPa to 1300 MPa, respectively as the Ni content increased from x = 0 to 10 at. %. Further, these alloys showed better wear resistance and biocompatibility as compared to 316 L.

Refractory high entropy of alloys

The refractory high entropy alloys (RHEAs) are an important class of HEAs mainly consisting of refractory elements like Ti, V, Cr, Zr, Nb, Mo, Y, W etc. In the year 2011, Senkov and Miracle [21] propagated the idea of RHEAs with their initial work on MoNbTaTiW based systems. Understanding the structure, microstructure, and thermal stability of these HEAs are of utmost importance for its potential application for high temperature structural materials. We will discuss the structural and microstructural stability in two RHEA systems

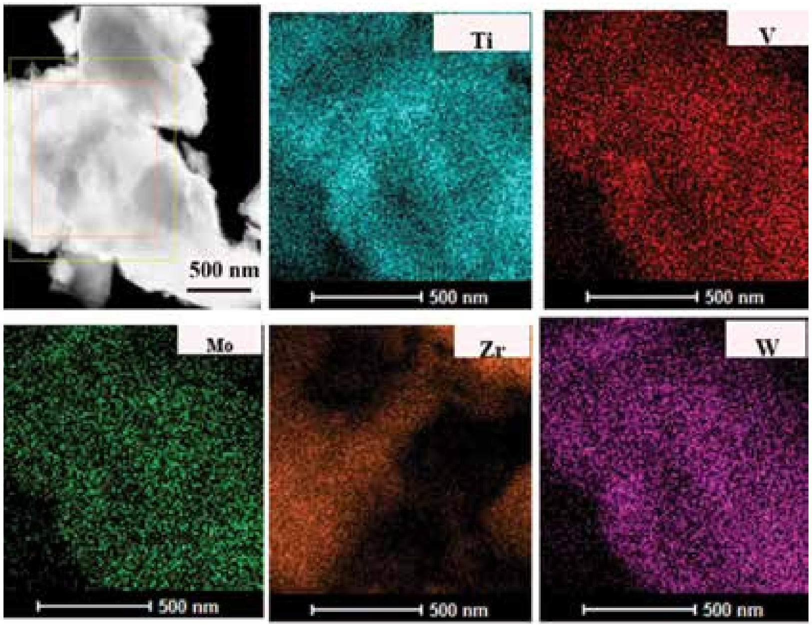

Fig. 10 : STEM-EDS analysis of the as-cast powdered sample. The oval and rectangular area marked on Ti and Zr are showing lean regions in the elemental mapping [22].

from our work i.e. TiVZrMoW [22] and TiVZrYHf. The prediction of phases in TiVZrMoW RHEAs was attempted theoretically by following (i) Semi-empirical Miedema model, (ii) an 8 atom SQS generated using ATAT software, and the enthalpy of mixing value for the structure (FCC, BCC and HCP) calculated using DFT and (iii) CALPHAD approach. The as-cast alloy shows the presence of major BCC1 (a = 3.17 ± 0.02 Å) being Mo and W rich and minor BCC2 (a = 3.65 ± 0.02 Å) being Ti, Zr rich along with C15 type ternary Zr $(Mo, W)_2$ Laves phase (a = 7.58 ± 0.02Å).

Figure 10 discerns the elemental distribution of alloying elements in these RHEA. The Ti, Zr rich regions and Mo, W rich regions were clearly seen in the STEM-HAADF-EDS map. The DSC analysis of the as-cast sample shows two endothermic peaks of solid-solid transformation up to 620°C. However, the alloy does not show any transformation in the temperature range of 620 - 1000°C. The annealed sample (at 900°C) shows that two BCC phases present in the as-cast sample were transformed into the ordered B2 structure.

The DFT approach in the study of phase stability of second refractory alloy, i.e., TiVZrYHf is a variation of cluster expansion method with fixed composition and cell size. Enthalpy of mixing of BCC and HCP structures were calculated for the distinct configuration of atoms on the lattice sites using a ten-atom cell. The annealed alloy was examined by XRD, SEM, and SEM-EDS. The annealed sample shows the presence of two disordered HCP1 (a = 3.18 ± 0.02 Å, c/a = 1.58) and HCP2 (a = 3.67 ± 0.02 Å, c/a = 1.55), along with BCC (a = 3.16 ± 0.02 Å) and the ordered (Hf, Zr)V2 (C15 type Laves phase, a = 7.41 ± 0.02 Å) phase which is in accordance to the theoretically predicted phases. The SEM-EDS mapping of the annealed sample shows that the major HCP1 phase contains Hf and Zr predominantly along with some Ti.

Multi-component high entropy intermetallics and Al-HEA composites

This is a new class of HEAs, that has gained a lot attention off-late. Here, we will be discussing some of our recent work on multi-component high entropy intermetallics systems i.e., Laves phase, sigma phase, γ-brass alloys. The first report on the single-phase multi-component TiZrVCrNi high entropy Laves phase was reported earlier by us in 2017 [23,24]. This TiZrVCrNi HEA prepared by the conventional melting and casting as well as by the melt-spinning technique, exhibits micron size hexagonal C14 type Laves phase and nanocrystalline Laves phase respectively [23]. The detailed characterisation by X-ray diffraction, scanning and transmission electron microscopy and energy-dispersive X-ray spectroscopy confirmed the existence of a single-phase multi-component hexagonal C14-type Laves phase in all the as-cast, melt-spun and annealed alloys. The lattice parameter a = 5.08 Å and c = 8.41 Å was determined from the annealed material (annealing at 1173 K). The thermodynamic calculations following the Miedema's approach support the stability of the high-entropy multicomponent Laves phase compared to that of the solid solution or glassy phases. These high entropy intermetallics represents excellent hardness (~8.92 GPa at 25g load) for nanocrystalline high-entropy alloy ribbon without any visible signature of cracking. It implies that these high entropy intermetallics have a high-yield strength (~3.00 GPa) with reasonable fracture toughness. Further, we have investigated the hydrogen storage properties of TiZrVCrNi high entropy intermetallics [25]. The alloy investigated for hydrogen storage was synthesized by vacuum arc melting having a C14 type hexagonal Laves phase. The pressure composition isotherms (PCI) of this alloy were investigated with pressure ranges at 0-40 atmosphere (Figure 11). The total hydrogen storage capacities were found to be 1.52 wt. %.

The reversible hydrogen storage capacity was quite stable and only slight decreases in the storage capacity was observed after 10 cycles during hydrogen soaking. The demonstrations of hydrogen storage capacity of the TiZrVCrNi equiatomic alloy were found to be very promising and surge the path for potential hydrogen storage application of these high entropy intermetallics with Laves phases.

The multi-component σ-phase (sigma phase) were observed in Cantor based HEAs prepared by mechanical alloying followed by pressure-less

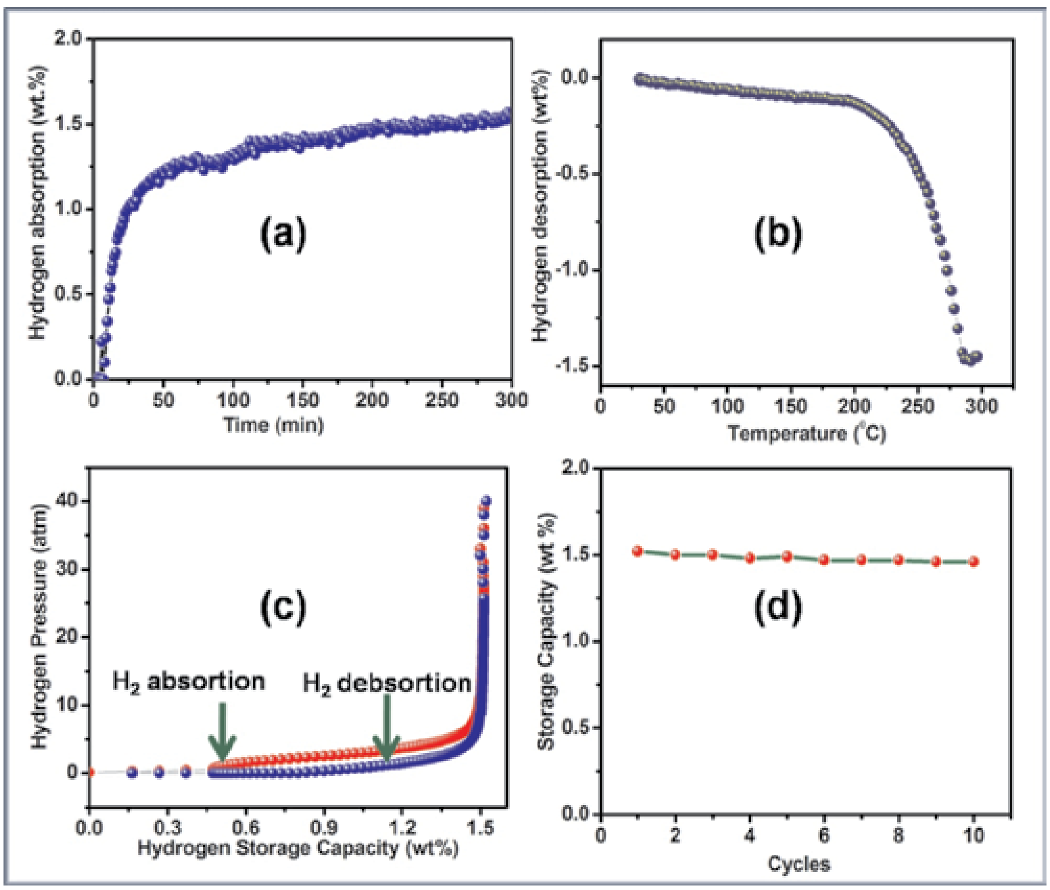

Fig. 11 : Hydrogenation curve of bulk as-cast $Ti_{20}Zr_{20}V_{20}Cr_{20}Ni_{20}$ HEA, (b) TPD curves of hydrogenated kinetics curve of bulk as-cast $Ti_{20}Zr_{20}V_{20}Cr_{20}Ni_{20}$ HEA, (c) pressure composition isotherm curve for absorption and desorption of bulk as-cast $Ti_{20}Zr_{20}V_{20}Cr_{20}Ni_{20}$ HEA and (d) Number of Cycles vs. hydrogen storage capacity of bulk as-cast $Ti_{20}Zr_{20}V_{20}Cr_{20}Ni_{20}$ HEAupto10 cycles [25].

sintering at elevated temperatures in CrMnFeCoMo system. The 40 h milling resulted in the formation of two solid solution phases with BCC structure (a= 3.146 ± 0.002 Å and 2.873 ± 0.002 Å) along with minor amount of retained α-Mn [26]. Phase formation, chemical composition, thermal stability etc. were also evaluated using electron microscopy and differential thermal analysis (DTA) methods as well as in-situ high temperature x-ray diffraction technique. The pressure-less sintered sample exhibited four phases i.e. two BCC solid solution, σ (sigma) and μ (mu), which were found to be stable until melting of these alloys. The phase formation was predicted by Thermo-Calc approach and was compared with the experimental observation as well as other calculated results. The sintered samples were tested by instrumented hardness tester for evaluation of mechanical properties, and was found to exhibit high hardness (9.3 ± 0.3 GPa) and Young's modulus (~245 ± 6 GPa).

Similarly, effort was made to synthesize Al- HEA (AlSiCrMnFeNiCu) composite by powder metallurgy route. The high entropy (AlSiCrMnFeNiCu) phase was found to have a major B2-type phase (a=0.29 nm; cP2) along with a minor phase corresponding to Cr_5Si_3-type silicide (a=b=0.9165 nm, c=0.4638 nm; tI32). These high entropy aluminides were found to have excellent hardness (~7 GPa) with a low-density of 5.08 $g.cm^{-3}$, making them lucrative to be exploited as a reinforcement for Al matrix composites. We have demonstrated the synthesis of 6082 Al matrix composite reinforced with AlSiCrMnFeNiCu high entropy aluminide by mechanical milling followed by pressure-less sintering. Mechanical milling (MM) imparts significant refinement, and nanostructuring of grains (~10–12 nm) for Al based nanocomposite powder was observed (Figure 12).

These powders of Al based nanocomposite was found to be thermally stable up to 650^0C. Further, these Al-HEA nanocomposite powders were consolidated through pressure-less sintering at 560^0C, which led to the formation of a thin ~400–500 nm transitional layer at the interface. The microhardness of these AMCs was tuned in the range of~0.90 to 1.81 GPa.

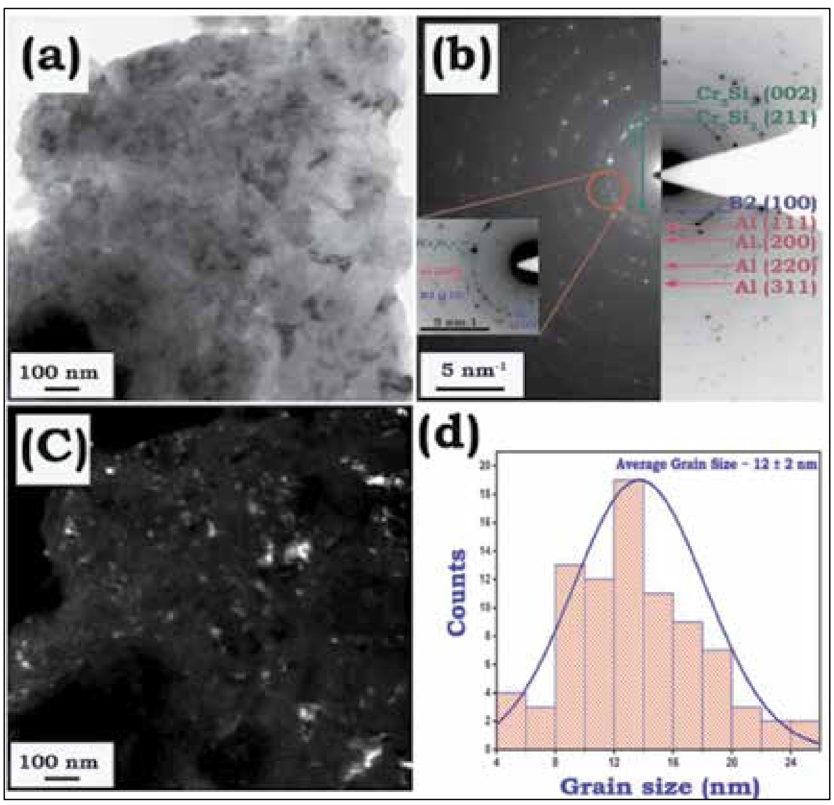

Fig. 12 : TEM micrograph of Al-30HEA nanocomposite showing the (a) bright-field image (b) corresponding selected area diffraction pattern, (c)dark field image, and (d) grain size distribution in nanocomposites [27].

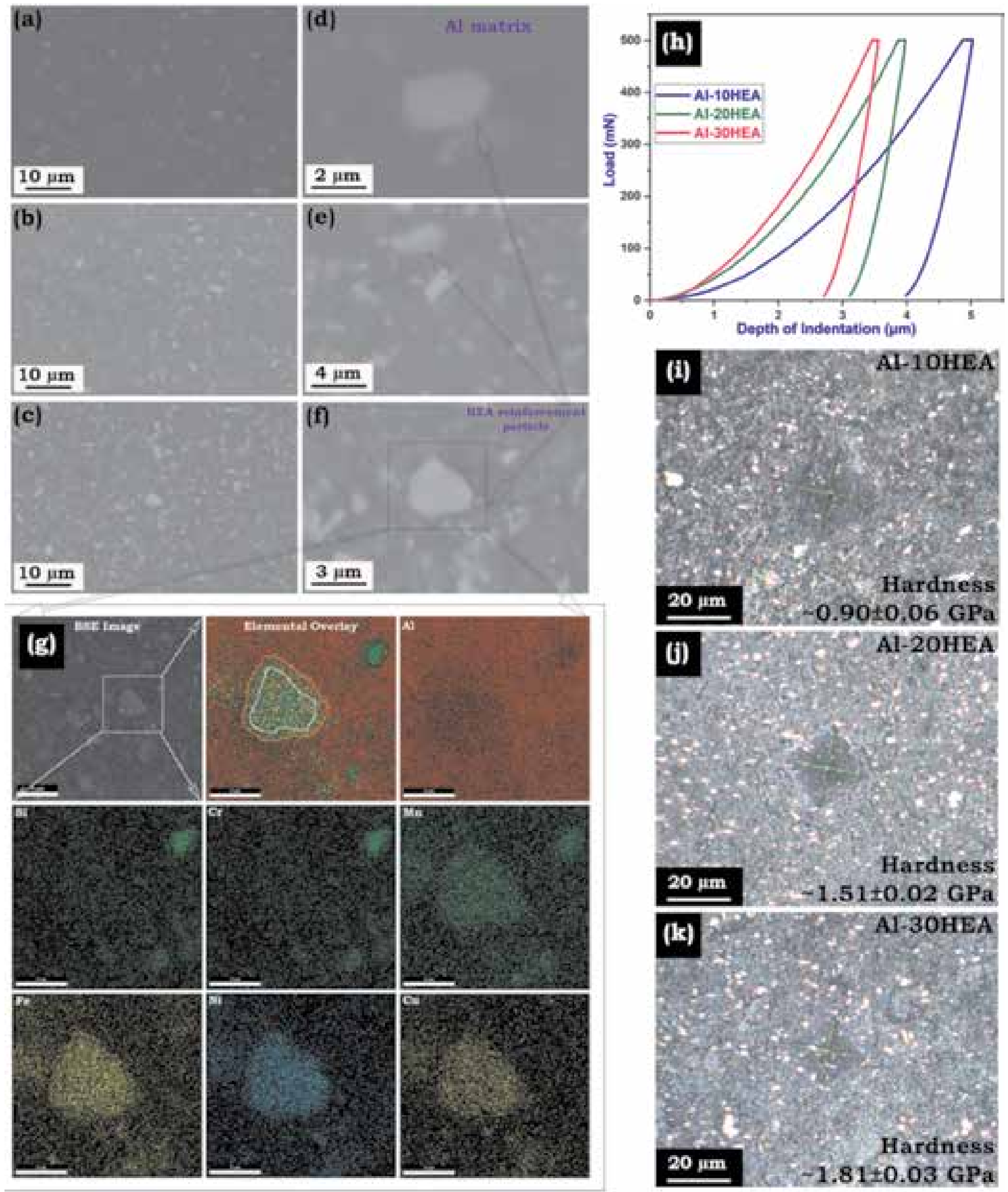

Fig. 13 : SEM micrograph of (a & d) Al-10HEA, (b & e) Al-20HEA, (c & f) Al-30HEA consolidated by pressure-less sintering at different magnification. (g) SEM–EDS mapping of Al-30HEA composite consolidated by pressure-less sintering showing the formation of transitional layer and elemental distribution. (h) Load versus indentation depth plot for Al-HEA composite. Optical micrograph for the indentation on (i) Al-10HEA (j) Al-20HEA, and (k) Al-30HEA pressure-less sintered composite [27].

Fe-based medium entropy alloys

At the early stage of the development of high-entropy alloys (HEAs), the focus was centered on producing alloys with simple solid solution phases of BCC, FCC and HCP phases to utilize the concept of configurational entropy. Later on, it was realized that the maximization of the configurational entropy through the equiatomic composition of the constituent elements is not the sole parameter to form the random solid solution. The non-equiatomic alloy composition provides more flexibility in designing the new alloys in the vast composition space and utilizes the effect of chemical composition on the microstructural evolution, which will lead to enhanced properties. This also allows designing alloys to reduce the material cost, to meet the applicability of these alloys.

In this regard, the element Fe draws more attention due to conventional Fe-based alloys have shown an excellent set of properties. With this objective, we have developed two Fe-based medium entropy alloys (MEAs) of 1.5 Kg weight each through vacuum induction melting furnace. The first composition of $Fe_{40}Cr_{25}Ni_{15}Al_{15}Co_5$ MEA in the as-cast state has shown the two-phase structure of Fe-Cr rich BCC phase and Ni-Al rich ordered B2 phase. The bright field and corresponding selected area diffraction (SAD) pattern of the as-cast alloy are given in Figure 14. The cuboidal B2 precipitates of sizes 100-200 nm are embedded within the disordered BCC matrix. In the diffraction pattern (Figure 14 (b)), a cubic pattern with a four-fold rotation symmetry is easily discerned. Additionally, modulation of intensity among the diffraction spots are present which may be due to the partial or complete ordering of either the B2/BCC phase or both phases simultaneously.

The orientation relationship is [100] of the B2 phase is parallel to the [100] of the BCC phase and the [110] of the B2 phase is parallel to the [110] of the BCC phase. This is commonly known as a cube-on-cube orientation relationship with no in-plane rotation. Under this situation, the interface between the cuboid and the matrix is likely to be (100) type. A closer view of the B2 precipitates with the BCC matrix can be seen through a magnified image (Figure 14 (c)). Figure 14 (c & d) shows the bright field and dark field imaging of the B2 precipitate with the matrix. The presence of the dislocation lines could be observed in the B2 phase and the BCC matrix in the bright field as well as in the dark field image. The appearance of the dislocation lines indicates that they are most likely mixed type. The presence of the thickness fringes at the interface of the cuboids further confirms the polyhedral nature of the precipitates. While some of the dislocations end at the BCC-B2 interface, some dislocations do cross over the interface. This is probably due to the semi-coherent nature of the interface.

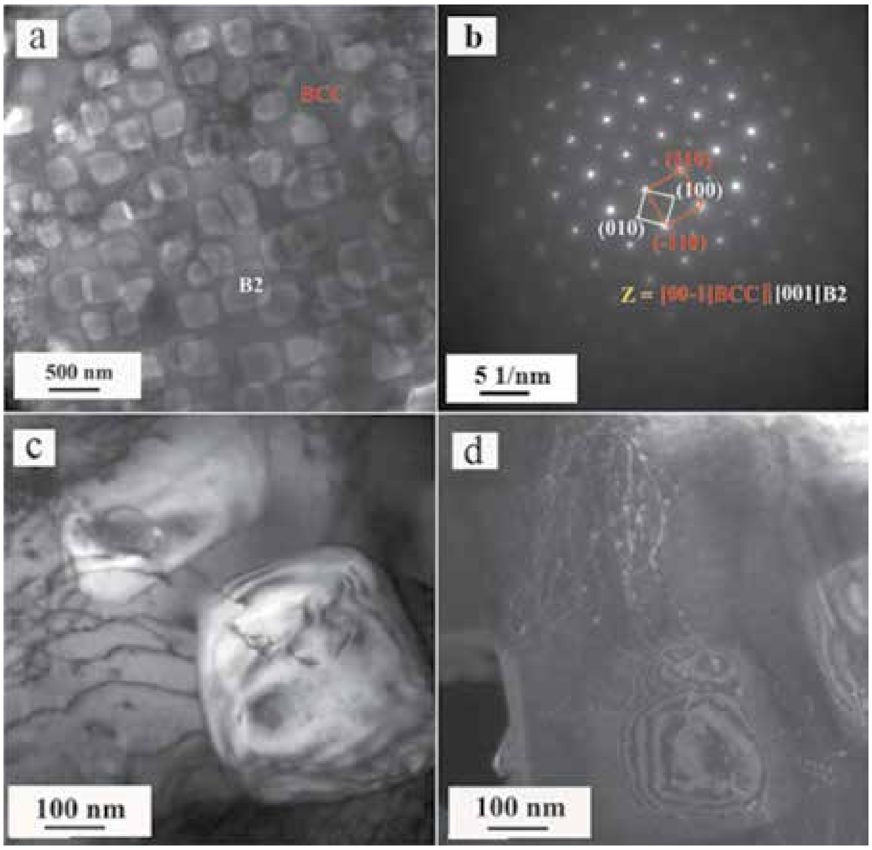

Fig. 14 : (a) Bright field electron micrograph and (b) selected area diffraction pattern (SAD) of as-cast Fe40Cr25Ni15Al15Co5 MEA. Cuboidal B2 precipitates are embedded in the BCC-disordered matrix. (c) & (d) bright and dark field images of B2 precipitates within the disordered BCC matrix [28].

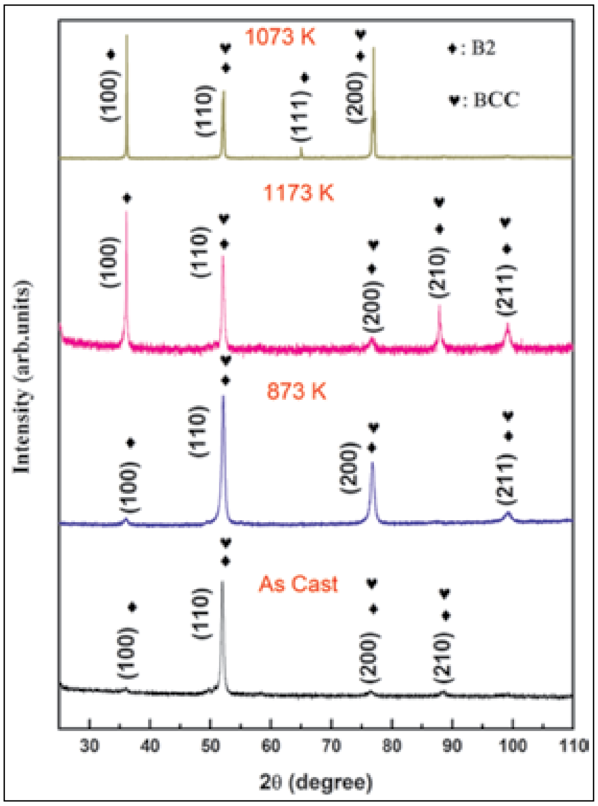

Fig. 15 : X-ray diffraction patterns of (a) as-cast and (b) heat-treated samples at 600 ^{0}C (873K), 900 ^{0}C (1173 K) - 2h & 800 ^{0}C (1073 K) for 12h and cooled down in a furnace [28].

The phase stability of the alloy was studied by exposing the as-cast alloy at different temperatures. Figure 15 shows the multiple displays of X-ray diffraction patterns at different time-temperature scales. It can be seen that at 600 ^{0}C (873K) there was no change in the phase observed except the increase in intensities of the peaks. This may happen due to the release of the crystal strain during the heat treatment of the alloy. Further increase in heating temperature at 800 ^{0}C (1173K), shows the increase in the intensity of the first superlattice reflection (100) of the B2 phase, relative to the as-cast structure.

This suggests that with the increase in heat treatment temperature degree of ordering increases. It means the volume fraction of the B2 phase is increased. The thermal stability of the evolved phases was further investigated at a longer holding time of 12h at 800 ^{0}C (1073K). There was no sign of phase transformation that could be observed even at a longer holding time. The diffraction pattern corresponding to this temperature showed all the reflections of the B2 phase. Therefore, it is imperative to say that the B2-type ordered phase is stable over a higher time-temperature range. The alloy is found to have a yield strength of ~ 1012 MPa and an ultimate compressive strength of ~1405 MPa. The yield strength of the studied alloy is comparatively higher than some of the earlier reported HEAs, but the alloy lacks plasticity. This may be due to the presence of the brittle Ni-Al-based B2-type intermetallic phase.

In the second composition of $Fe_{50}Mn_{20}Al_{15}Ni_{10}Co_5$ MEA, we incorporate the Mn to further reduce the cost and induce the FCC phase-forming ability of the alloy. The as-cast alloy shows the BCC/B2 phase along with the formation of the FCC phase near the grain boundary area. Figure 3 shows the high-magnification SEM micrographs. The marked areas, near the grain boundary and in the matrix (white contrast) region, in Figure 16 (a) were magnified. The region near the grain boundary has black contrast and appears in the form of fine leafs (figure 16 (b). This might be the case of the rejection of Fe and Mn elements during the formation of Al-Ni-rich B2 precipitates in the BCC matrix. The formation of

FCC (dark contrast) would lead to the rejection of Al and Ni into the matrix, which favours the B2 phase formation. A closer look at the same magnified area in Figure 16 (c) further reveals that the regions away from the dark area possess very fine structures. Similarly, a high magnification micrograph of the white matrix region (marked with a circle in Figure 16 (a)) depicts a modulated structure of densely formed B2 precipitates in the BCC matrix (figure 16 (d and e)). The SEM-EDS line analysis through the modulated structure confirms the Ni-Al-rich composition of the B2 precipitates (Figure 16 (f)).

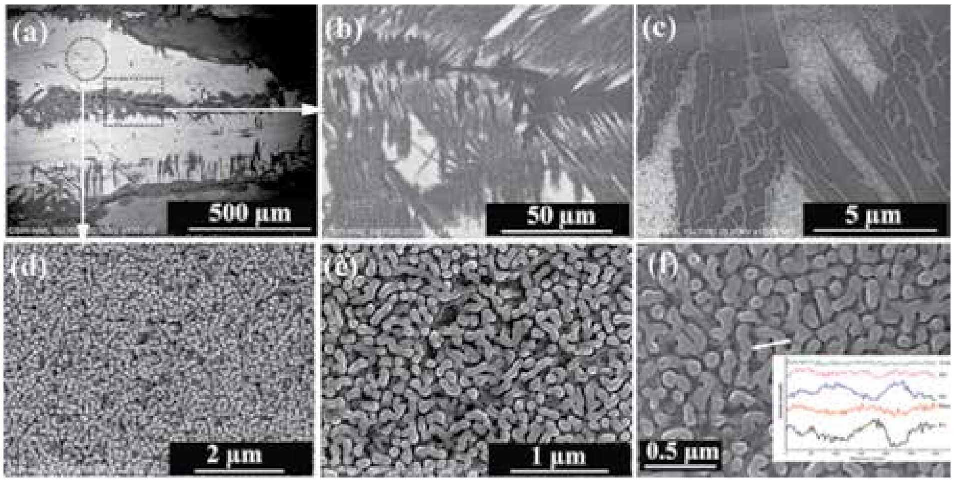

Fig. 16 : The high-resolution SEM micrographs of as-cast $Fe_{50}Mn_{20}Al_{15}Ni_{10}Co_5$ MEA. Marked rectangular FCC region magnified in (b) and (c). Marked circular BCC region magnified in (d, e and f). The EDS shown in the insert of (f) indicates the formation of the Ni-Al-rich B2 phase [29].

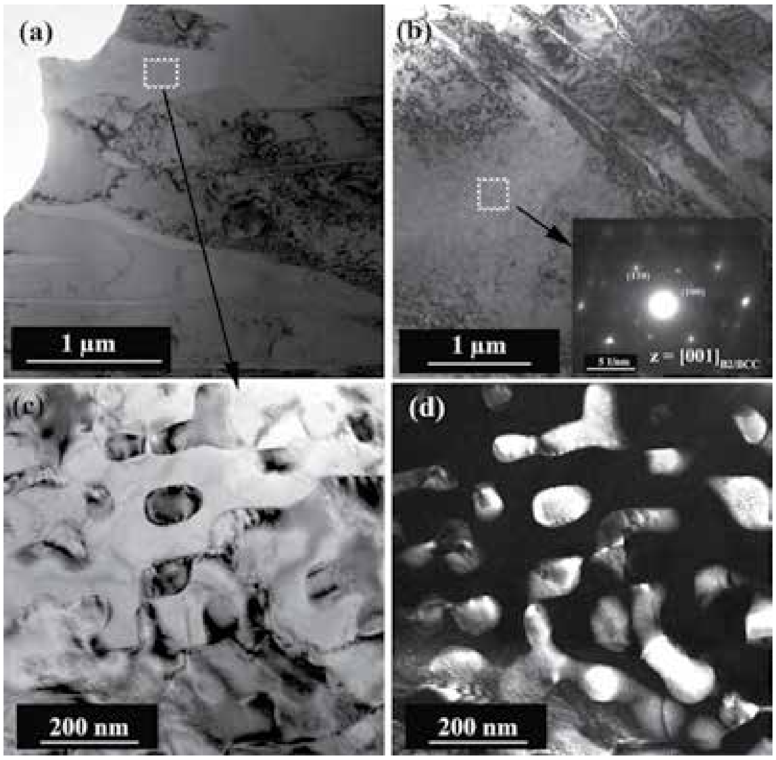

Fig. 17 : The bright field images (a and b) and selected area diffraction pattern of the marked area in (b) of as-cast $Fe_{50}Mn_{20}Al_{15}Ni_{10}Co_5$ MEA. The high magnification bright field and dark field image of the marked area in (a). B2 precipitates of varying sizes of range 80-100 nm could be observed in the BCC matrix [29].

Figure 17 shows the TEM bright field (BF) and dark field (DF) micrographs and the corresponding selected area diffraction (SAD) patterns of the alloy. The elongated grains of width in the sub-micron range and dark regions in the marked grains indicate the presence of defects in the alloy (Figures 17 (a) and (b)). The SAD patterns of the marked areas confirm the formation of ordered B2 (a= 2.93Å) and disordered BCC (a= 2.96Å) phase (Figure 17 (b) inset image). The marked area in the BF image (Figure 17(a)) indicates the formation of B2 precipitates in the BCC matrix. The dark field image shows that the width of B2 precipitates varies in the range of 80-120 nm of different shapes. The chemical compositions of ordered B2 precipitates in the disordered BCC matrix were confirmed through the STEM-EDS elemental maps. Figure 18 shows the STEM BF micrograph and corresponding elemental maps of Fe, Mn, Al, Ni and Co elements. It shows that B2 precipitates are significantly enriched in Ni and Al elements and depleted in Fe and Mn. Moreover, Co is uniformly distributed in both phases though with a slight enrichment in the B2 phase.

The mechanical properties of the as-cast alloy were evaluated at room temperature in terms of compression behvaiour and hardness. The alloy demonstrates the yield and ultimate compressive strength of ~1250 MPa and ~1675 MPa, respectively, with compressive ductility of ~42%. The alloy exhibited a high hardness value of ~450 HV in the as-cast condition. These above results have shown the partial substitution of constituent elements into Fe, provides immense opportunities to design the alloys for high-temperature applications along with balance of strength and ductility. Although the cost of the Fe-based MEAs is still higher compared to the conventional steel, it has shown a relatively lower cost compared to the other equiatomic HEAs and MEAs. The development of Fe-based MEAs has given a potential direction for the future development of MEAs to meet the industrial application of these alloys.

Concluding Remarks

While designing alloys suitable for technological applications based on structural and functional properties, it is suggested that HEAs could be taken as the base alloy and then minor additions could be made to obtain the desired microstructure and mechanical properties for improving the stability and the properties. It is important to emphasize that attention of materials researchers have been focused at the central or near central region of the phase diagram, which was otherwise grossly

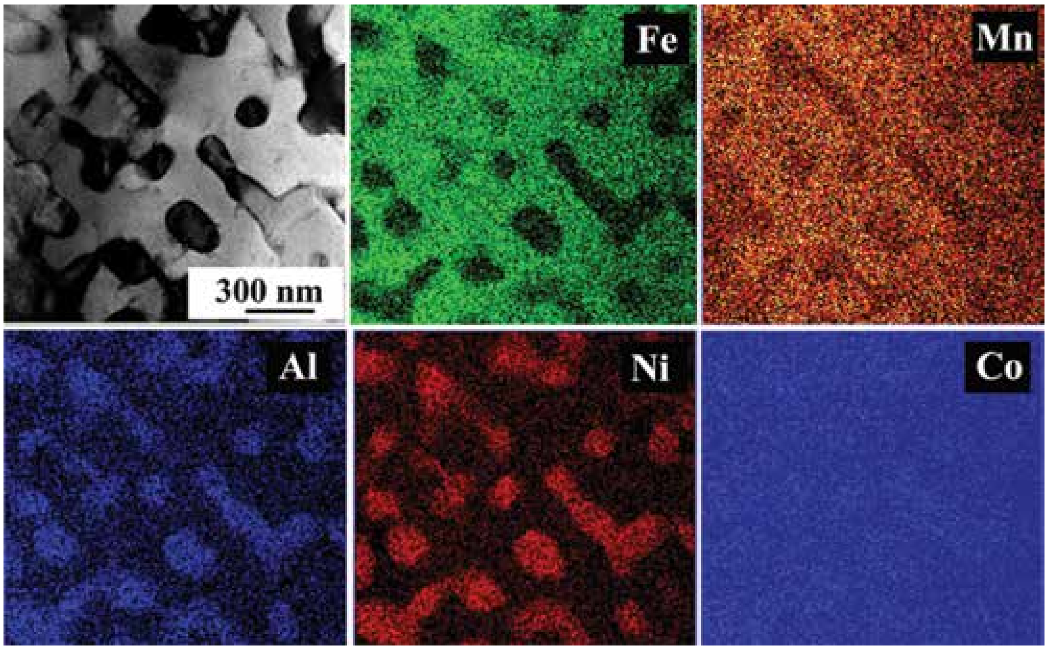

Fig. 18 : The STEM-EDS elemental maps of the as-cast $Fe_{50}Mn_{20}Al_{15}Ni_{10}Co_5$ MEA. The B2 precipitates richer in Ni and Al, and the BCC matrix richer in Fe and Mn could be depicted. However, Co is ingressed in both phases [29].

ignored so far except a few cases. However, it has also raised the question of the effective role and ability of configurational entropy to stabilize the useful solid solubility range of the disordered solid solution phases. It has now become clear that the alloy design strategy of combining multiple elements in near-equiatomic or non-equiatomic proportions with single or multi-phase combination has tremendous potential for developing novel materials under the category of HEAs. However, there are several unresolved matters related to elemental distribution, exact calculation of phase selection, phase stability at lower temperature, exact contribution and measurement of configurational entropy, phase separation, role of misfit strain and its estimation at the level of nano- and microscale and structural applications. The deformation science and the role of nanotwins and dislocations in the presence of strain due to multicomponent solutes need to be understood. It has been recently emphasized that the HEA-based design strategy should not be restricted to single-phase solid solutions alone and it should be extended to a wide range of complex phases including intermetallics as well as developing composites for exploiting the renaissance in physical metallurgy realized in recent times. In order to reap the benefit of this new class of materials, it has been suggested to explore the possible application of HEAs in three strategic areas – advanced ultra super critical (AUSC) coal-powered station, radiation environment, and aero-gas turbine engines. There are also attempts being pursued to develop high entropy ceramics and polymeric materials and composites for enhanced structural and functional properties and their applications. It is anticipated that these continuous and intense research efforts on multiprincipal multielement materials will lead to advance our fundamental understanding on the concentrated alloys and also to develop some useful materials for the niche applications.

Acknowledgements

I would like to record my deep sense of gratitude to Prof. S. Ranganathan, Prof. K. Chattopadhyay, Prof S. Lele, (Late) Prof. O.N. Srivastava, (Late) R. Krishnan, Prof. I. Manna, and Prof. B.S. Murty for their continuous encouragements and support throughout my academic journey. My heartfelt thanks are due to all my collaborators and colleagues, especially, Prof. R.K. Mandal, Prof. B.N. Sarma, Dr. Joysurya Basu, Dr. R. Manna, Dr. Kausik Chattopadhyay, Dr. T.P Yadav and Dr. V.C. Srivastava for their active collaboration and many stimulating discussions. I also wish to convey my sincere thanks to all my former and current students who were the driving force to motivate me to continue the work, especially, Dr. Vikas Shivam, Dr. Vivek Pandey, Dr. Nandini Singh, Dr. Yagnesh Shadangi, Mr. Harsh Jain, Mr. Priyotosh Pradhan, Mr. Abhisek Singh, Mr. Ritik Roshan Tripathy, and Mr. Rajat Gupta. I thankfully acknowledge the efforts of Dr, Yagnesh Shadangi and Dr. Vikas Shivam in assisting me to prepare this article. On this occasion, I would like to thank my wife, Prof. Santwana Mukhopadhyay and my daughter, Semanti and also other family members for their continuing support, understanding and adjustments during all seasons of my life.

References (selected)

[1] J.W. Yeh, S.K. Chen, S.J. Lin, J.Y. Gan, T.S. Chin, T.T. Shun, C.H. Tsau, S.Y. Chang, Nanostructured high-entropy alloys with multiple principal elements: Novel alloy design concepts and outcomes, Adv. Eng. Mater. **6** (2004) 299–303.

[2] B. Cantor, I.T.H. Chang, P. Knight, A.J.B. Vincent, Microstructural development in equiatomic multicomponent alloys, Mater. Sci. Eng. A. **375–377** (2004) 213–218.

[3] S. Ranganathan, Alloyed pleasures: Multiatomic cocktails, Curr. Sci. **85** (2003) 1404–1406.

[4] B.S. Murty, J.W. Yeh, S. Ranganathan, High Entropy Alloys, Butterworth-Heinemann, 2014.

[5] N.K Mukhopadhyay, High entropy alloys: a renaissance in physical metallurgy, Curr. Sci. **109** (2015) 665–667.

[6] J.W. Yeh, Alloy design strategies and future trends in high-entropy alloys, JOM. **65** (2013) 1759–1771.

[7] M. Vaidya, G.M. Muralikrishna, B.S. Murty, High-entropy alloys by mechanical alloying : A review, J. Mater. Res. **34** (2019) 664–686.

[8] V. Shivam, J. Basu, V.K. Pandey, Y. Shadangi, N.K. Mukhopadhyay, Alloying behaviour, thermal stability and phase evolution in quinary AlCoCrFeNi high entropy alloy, Adv. Powder Technol. **29** (2018) 2221–2230.

[9] V. Shivam, J. Basu, Y. Shadangi, M.K. Singh, N.K. Mukhopadhyay, Mechano-chemical synthesis,

thermal stability and phase evolution in AlCoCrFeNiMn high entropy alloy, J. Alloys Compd. **757** (2018) 87–97.

[10] A. Kareer, J.C. Waite, B. Li, A. Couet, D.E.J. Armstrong, A.J. Wilkinson, Short communication : ' Low activation , refractory , high entropy alloys for nuclear applications ,' J. Nucl. Mater. **526** (2019) 1–6.

[11] B. Cao, T. Yang, W. Liu, C.T. Liu, Precipitation-hardened high-entropy alloys for high-temperature applications : A critical review, MRS Bull. **44** (2019) 854–859.

[12] O. Maulik, D. Kumar, S. Kumar, D.M. Fabijanic, V. Kumar, Intermetallics Structural evolution of spark plasma sintered AlFeCuCrMg x (x=0, 0.5,1.0, 1.7) high entropy alloys, **77** (2016) 46–56.

[13] N. Singh, Y. Shadangi, G.S. Goud, V.K. Pandey, V. Shivam, N.K. Mukhopadhyay, Fabrication of MgAlSiCrFe Low-Density High-Entropy Alloy by Mechanical Alloying and Spark Plasma Sintering, Trans. Indian Inst. Met. **74** (2021) 2203–2219.

[14] N. Singh, Y. Shadangi, N. Krishna, Phase Evolution and Thermal Stability of Low-Density MgAlSiCrFe High-Entropy Alloy Processed Through Mechanical Alloying, Trans. Indian Inst. Met. **73** (2020) 2377–2386.

[15] N. Singh, Y. Shadangi, V. Shivam, N.K. Mukhopadhyay, MgAlSiCrFeNi low-density high entropy alloy processed by mechanical alloying and spark plasma sintering: Effect on phase evolution and thermal stability, J. Alloys Compd. **875** (2021) 159923.

[16] V.K. Pandey, Y. Shadangi, V. Shivam, J. Basu, K. Chattopadhyay, B. Majumdar, B.N. Sarma, N.K. Mukhopadhyay, Synthesis, Characterization and Thermal Stability of Nanocrystalline MgAlMnFeCu Low-Density High-Entropy Alloy, Trans. Indian Inst. Met. **74** (2021) 33–44.

[17] D. Raabe, C.C. Tasan, H. Springer, M. Bausch, From High-Entropy Alloys to High-Entropy Steels, Steel Res. Int. **86** (2015) 1127–1138.

[18] H. Jain, Y. Shadangi, D. Chakravarty, K. Chattopadhyay, A.K. Dubey, N.K. Mukhopadhyay, Low-density Fe40Mn19Ni15Al15Si10C1 high entropy steel processed by mechanical alloying and spark plasma sintering: Phase evolution, microstructure and mechanical properties, Mater. Sci. Eng. A. **869** (2023) 144776.

[19] H. Jain, Y. Shadangi, V. Shivam, D. Chakravarty, Dibyendu Mukhopadhya, N.K Kumar, Phase evolution and mechanical properties of non-equiatomic Fe-Mn-Ni-Cr-Al-Si-C high entropy steel, J. Alloys Compd. **834** (2020) 155013.

[20] H. Jain, Y. Shadangi, D. Chakravarty, A.K. Dubey, N.K. Mukhopadhyay, High entropy steel processed through mechanical alloying and spark plasma sintering: Alloying behaviour, thermal stability and mechanical properties, Mater. Sci. Eng. A. **856** (2022) 144029.

[21] O.N. Senkov, G.B. Wilks, J.M. Scott, D.B. Miracle, Mechanical properties of Nb 25 Mo 25 Ta 25 W 25 and V 20 Nb 20 Mo 20 Ta 20 W 20 refractory high entropy alloys, Intermetallics. **19** (2011) 698–706.

[22] V.K. Pandey, Y. Shadangi, V. Shivam, B.N. Sarma, N.K. Mukhopadhyay, Theoretical and experimental study on phase stability of TiVZrMoW refractory high entropy alloy, Philos. Mag. **102** (2022) 480–503.

[23] T.P. Yadav, S. Mukhopadhyay, S.S. Mishra, N.K. Mukhopadhyay, O.N. Srivastava, Synthesis of a single phase of high-entropy Laves intermetallics in the Ti–Zr–V–Cr–Ni equiatomic alloy, Philos. Mag. Lett. **97** (2017) 494–503.

[24] O.N. Senkov, G.B. Wilks, D.B. Miracle, C.P. Chuang, P.K. Liaw, Intermetallics Refractory high-entropy alloys, Intermetallics. **18** (2010) 1758–1765.

[25] A. Kumar, T. Prasad, N. Krishna, Notable hydrogen storage in Ti-Zr-V-Cr-Ni high entropy alloy, Int. J. Hydrogen Energy. **47** (2022) 22893–22900.

[26] P. Pradhan, Y. Shadangi, V. Shivam, N.K. Mukhopadhyay, Powder metallurgical processing of CrMnFeCoMo high entropy alloy_ Phase evolution, microstructure, thermal stability and mechanical properties, J. Alloys Compd. **935** (2023) 168002.

[27] Y. Shadangi, K. Chattopadhyay, N.K. Mukhopadhyay, Powder metallurgical processing of Al matrix composite reinforced with AlSiCrMnFeNiCu high-entropy alloys: Microstructure, thermal stability, and microhardness, J. Mater. Res. **38** (2023) 248–264.

[28] V.Shivam, J.Basu, R.Manna, N.K.Mukhopadhyay, Local Composition Migration Induced Microstructural Evolution and Mechanical Properties of Non-equiatomic Fe40Cr25Ni15Al15Co5 Medium-Entropy Alloy, Metall. Mater. Trans. A. **52** (2021) 1777–1789.

[29] V. Shivam, S. Kar, G.K. Bansal, A.K. Chandan, B.K. Sahoo, G.K. Mandal, N.K. Mukhopadhyay, V.C. Srivastava, A novel Fe-rich non-equiatomic medium-entropy alloy with superior mechanical properties, J. Alloys Compd. **952** (2023) 170029.

****


परमाणु रिएक्टर Nuclear Reactors
BWRs, PHWRs & FBRs
रक्षा Defence
अंतरिक्ष Space
थर्मल, Thermal,
उर्वरक & Fertilizer &
पेट्रोकेमिकल Petrochemical
अनुप्रयोग
APPLICATIONS
परमाणु उत्पाद
NUCLEAR PRODUCTS
राष्ट्र की सेवा में परमाणु
एन एफ सी
NFC
ATOMS IN THE SERVICE OF THE NATION
ट्यूबलर उत्पाद
TUBULAR PRODUCTS
नाभिकीय ईंधन सम्मिश्र NUCLEAR FUEL COMPLEX
परमाणु ऊर्जा विभाग की एक इकाई A Unit of Department of Atomic Energy, भारत सरकार Govt. of India
(आई.एस.ओ.9001, 14001 & 45001 संगठन ISO 9001, 14001 & 45001 Organization)
भारत के शांतिपूर्ण परमाणु कार्यक्रम को बढ़ावा देना Fuelling India's peaceful Nuclear program
महत्वपूर्ण उत्पादन और परीक्षण सुविधाएं
IMPORTANT PRODUCTION AND TESTING FACILITIES
Hot Extrusion
Pilger Mill
Vacuum Annealing
Sintering Furnaces
Bright Annealing Furnace
Robotic End Plate Welding
Ultrasonic - RP
Ultrasonic - RT
PRODUCTS: Nuclear Grade Fuels and Stucturals, Special and High purity materials, Special seamless tubes
SERVICES : Vacuum Arc Melting, Extrusion, Pilgering, Heat Treatment, Material Finishing, Bar and Wire drawing, U-Bending and Shot peening of Tubes, TIG/EB weld fabrication, Tools Fabrication, Developmen of Spl. Eqpt. Material Inspection, NDT, Chemical Analysis
हमारे उत्पादों और सेवाओं के व्यापक दृष्टिकोण के लिए, कृपया देखें For a comprehensive view of our products and services,
please visit www.nfc.gov.in
नाभिकीय ईंधन सम्मिश्र, हैदराबाद, भारत NUCLEAR FUEL COMPLEX, ECIL P.O. Hyderabad, TELANGANA, INDIA-500 062
Ph.: +91-40- 2712 1239 / 2718 4224, Fax: +91-40- 2712 1209 E-mail: marketing@nfc.gov.in

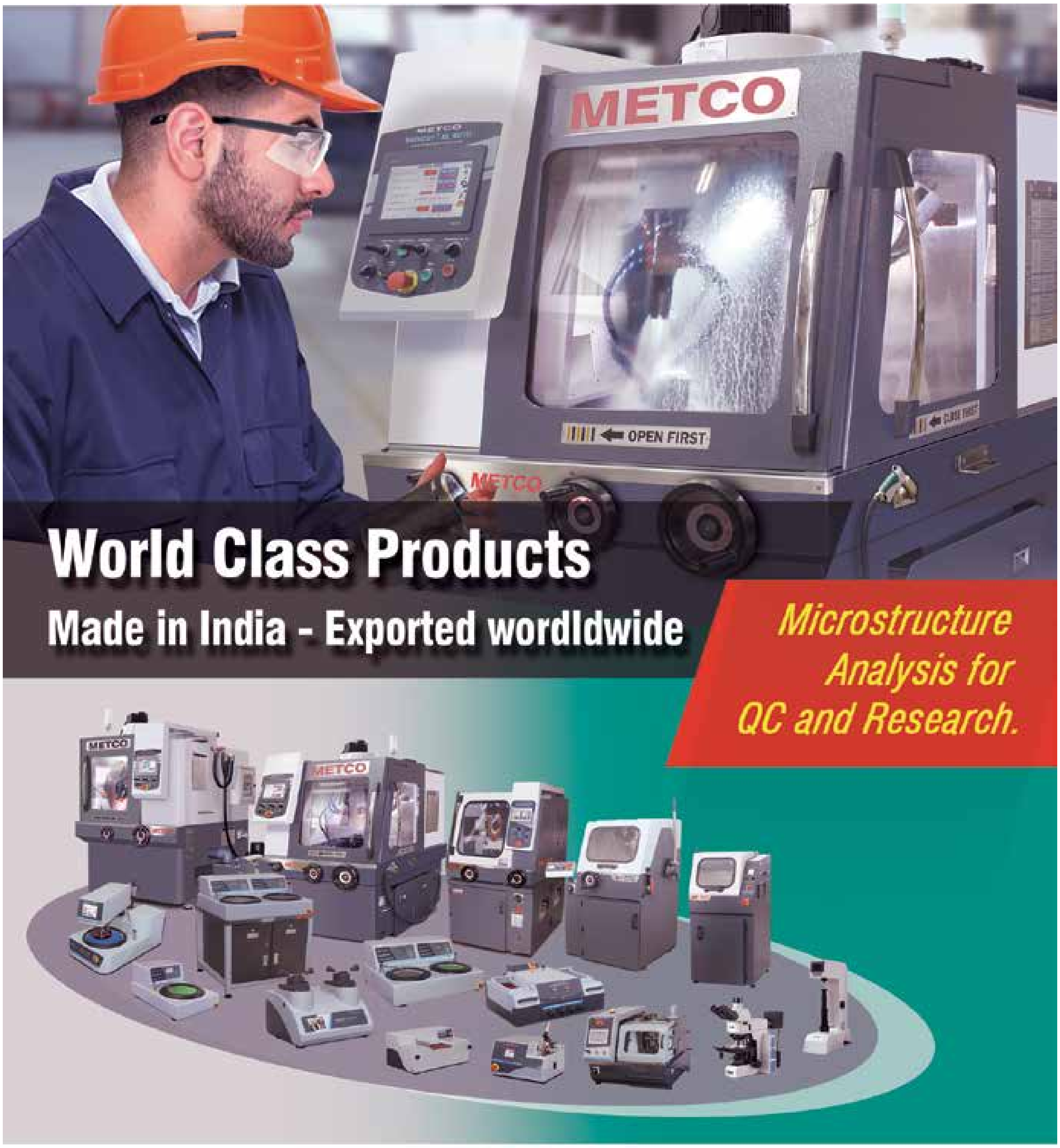
METCO
OPEN FIRST
World Class Products
Made in India - Exported wordldwide
Microstructure Analysis for QC and Research.
METCO

News Updates Domestic

RINL plans to trim its debt by selling UP wheel plant to Railways

State-owned Rashtriya Ispat Nigam Limited (RINL) plans to trim its debt by selling its Raebareli forged wheel plant to the Indian Railways, said a senior government official.

"The Indian Railways will pay RINL for the Raebareli wheel plant. This will help trim debt of the steel public sector undertaking," the official told on condition of anonymity, adding that the national transporter is the front runner for the wheel plant due to the 30-year offtake assurance.

RINL's ₹2,350-crore forged wheel plant in Raebareli, Uttar Pradesh, has been on the block since 2022. It has the capacity to make 100,000 wheels and was built in collaboration with SMS Germany. "Concerns were raised about offering the plant with the offtake agreement to a private player. It has now been decided that the Indian Railways will be best positioned to own the plant while operations can be outsourced," said the official. The Indian Railways is supposed to pay a cost-plus price for the wheels produced by the plant under the agreement.

The Economic Times (16.01.2024)

More funds for steel sector under green hydrogen mission if required, says R K Singh

Union Minister R K Singh assured stakeholders that additional funds will be allocated for decarbonisation of the steel sector under National Green Hydrogen Mission, if required. Singh chaired a meeting of government and industry stakeholders of the iron and steel sector in order to discuss pilot projects under the mission, an official statement said.

Officials of Ministry of New & Renewable Energy, Ministry of Steel and industry representatives from the iron and steel sector participated in the deliberations.

The Union Power and New & Renewable Energy Minister said that the funds available under the mission should be used to develop technology for integration of hydrogen in steel making.

The Economic Times (24.01.2024)

Eye on green transition, slew of incentives in works for steel cos

India is considering a slew of incentives such as concessional finance and long-term loans for steel makers as it prepares for green transition in steel production to tackle the carbon taxation challenges, including Europe's Carbon Border Adjustment Mechanism (CBAM).

A top government official told that an integrated document that compiles recommendations made by dedicated task forces, set up to look at measures needed to decarbonise the domestic steel sector, will soon be floated for consultations. "The 13 task forces have given their recommendations. Their recommendations will be compiled into a single integrated document and floated for stakeholder public consultations," the official said.

The Economic Times (29.01.2024)

India's April-December steel imports hit five-year high as demand soars

India's steel imports touched a five-year high in the first nine months of the fiscal year to the end of March, turning the country into a net importer of finished steel, according to provisional government data seen by Reuters.

A spurt in economic activity and a revamp of broader infrastructure have turned India into a bright spot for both Indian and global steel makers. Unlike India, steel demand is slowing down in Europe and the United States.

India imported 5.6 million metric tons of finished steel between April and December, up 26.4% from a year earlier, the data showed.

Steel consumption in India, the world's second-biggest crude steel producer, jumped 14.8% to a six-year high of 100 million metric tons during the period, reflecting buoyant demand for the alloy in one of the world's fastest growing economies.

India's steel demand is likely to stay strong as the government expects economic growth will outpace the global economy in the next fiscal year.

India's steel mills have called for government interventions and safeguard measures against surging imports. But, the federal Ministry of Steel has resisted calls for curbs, citing strong local demand.

The Economic Times (30.01.2024)

****

Chapter Activities Kalpakkam, Bhubaneswar, Jamshedpur

Kalpakkam Chapter

Prof. G. Phanikumar, Department of Metallurgical and Materials Engineering, Indian Institute of Technology Madras had visited IGCAR on 23rd November 2023 and delivered a technical lecture organised by IIM Kalpakkam Chapter. The title of the talk was "Open source software for High Performance Computing towards realizing ICME".

In this lecture, Prof Phanikumar has illustrated a methodology to reduce the time scale for development of new products by combining the experiment and computation using the Integrated Computational Materials Engineering (ICME) approach. The results of ICME approach on the welding and additive manufacturing were explained. He had also described the possible use of open source software package 'Microsim' to compute the microstructure evolution in a verity of engineering materials using the phase field simulation technique.

Bhubaneswar Chapter

With the world population increasing at an alarming rate, the demand for ore minerals has reached unprecedented levels. However, the availability of highgrade ores is diminishing rapidly. As a result, the utilization of low-grade ores has become increasingly vital to meet the growing demand. Mineral processing is the only practical solution to upgrade and utilize these low-grade ores. Keeping this need in mind, the IIM Bhubaneswar Chapter collaborated with CSIR-IMMT, Bhubaneswar, to organize a five-day refresher course called "Fundamentals and Advances in Mineral Engineering" (FAME-2023).

The course aimed to help Plant Executives/ Engineers, Academicians, and R&D professionals gain knowledge and insights into the latest techniques and advancements in mineral engineering. The refresher course, which was held from 18-22 December 2023, proved to be a valuable learning experience for all the participants.

The refresher course was attended by approximately 33 delegates from a diverse range of organizations, including AM/NS India, Innocule Materials and Additives Private Limited, Next Track Engineering Pvt. Ltd., Maharashtra Minerals Corporation Limited, Geomysore Services India Pvt. Ltd., and JSW Steel Limited. The course was conducted by highly experienced resource persons from R&D organizations, academic institutions, and industries.

The coursework covered a wide range of topics, starting from the fundamentals of geology to mineral resources, mineralogy, mineral characterization, comminution, gravity concentration, magnetic and electrostatic separation, flotation, pelletization, briquetting, flow sheet developments, value addition, and slurry transportation.

The participants were also given hands-on experience to deepen their knowledge of the subject. Overall, the course was conducted very smoothly, and the participants gained a comprehensive understanding of the topics covered.

Jamshedpur Chapter

TECHNICA 24, a National Symposium of Students of Metallurgical and Materials Engineering : TECHNICA 24, the annual national symposium of the students of the Department of Metallurgical and Materials Engineering organised at NIT Jamshedpur during January 25-27, 2024 by the NIT Jamshedpur in association with Indian Institute of Metals (IIM) Jamshedpur Chapter and Tata Steel Limited. TECHNICA is a unique forum where students from different institutes of national repute come together on one platform to showcase their technical expertise in the field of Metallurgy and Materials Engineering. Like every year, this year's event took place with the same enthusiasm as in previous years. Participants from various engineering institutions like BIT Sindri Dhanbad, Jadavpur University, BESU, NIAMT Ranchi and many more participated from other technical institutes in TECHNICA 24. It was held in the prestigious presence of organizations like RSB Global, Tata Steel, IIM Jamshedpur, National Metallurgical Lab, RS Rungta Groups, and many more. Every year, we introduce something new and captivating. This year's attractions include: Rhetorics: Language Arts Competition; Dr. DARA P Antia Metal Quiz: Metallurgy and Materials Science; Quizzica: Science and Technology General Knowledge Competition; Pictured: Photo Contest; Metallography contest, Poster Presentation and Magnum Opus: Technical Presentations Competition to enhance the fest's appeal. This year, we had over 100 participants from other colleges and over 200 registrations. On the inauguration day, the distinguished chief guest was Dr. Sandeep Ghosh Chaudhary, Chief Scientist at NML Jamshedpur. A special attraction was the visit to NML Jamshedpur and Ramakrishna Forging Ltd. We also organized a mental wellness program by ISKCON where Sri Prabhu Prem Swaroop Ji conducted a session for the students. The felicitation ceremony took place on January 27, 2024, with Mr. Biswajit Jena, RSB Jamshedpur Plant Head, as the chief guest. The valedictory program concluded with a vote of thanks Secretary Technica 24 and Socity of Metallurgical Engineering Students (SMES).

****

Head Office Activities

• IIM Secretary General Brig Arun Ganguli (Retd) visited IIM Bangalore Chapter on December 20, 2023 for the Membership drive.

• IIM HO bid farewell to the Sr. Manager (Membership) Ms. Indrani Ghosh at the Fort William Kolkata on January 5, 2024.

• IIM Secretary General Brig Arun Ganguli (Retd) and Mr. Tamal Goswami, Manager from IIM HO visited IIM Jamshedpur Chapter on January 16, 2024

Seminars & Conferences ICGSI 24

Tata Steel, in collaboration with The Indian Institute of Metals, Jamshedpur Chapter hosted a pivotal International Conference on Green & Sustainable Ironmaking on January 17-18, 2024, in Jamshedpur. The conference was inaugurated by key figures from Tata Steel and the Indian Institute of Metals. This event aims to address crucial themes related to decarbonization strategies within blast furnace operations, waste utilization, and advancements in ironmaking technologies. The conference highlighted cutting-edge methods in ironmaking. Key topics discussed included effective waste utilization, lower grade material use, and innovative carbon capture techniques. The conference emphasized the industry's shift towards Clever Carbon solutions, AI, and digital advancements in green steel production. Industry experts debated the future of green steel and strategies for achieving net-zero targets. A significant theme was the exploration of decarbonization in blast furnace operations. Dr. Ashok Kumar from Tata Steel, UK, and Christian Hoffman from Mckinsey, along with Dr Atanu Ranjan Pal, CTO of Tata Steel, delivered keynotes on these subjects. A panel discussion focused on benchmarking best practices for green steelmaking was also organized. The event united professionals in Direct Reduced Iron and blast furnace technology. Over 260 delegates, including technologists, researchers, and environmental advocates, participated.

Glimpses of ICGSI 24

****

Crude Steel Production Worldwide

2023 global crude steel production				
Rank	**Country**	**2023 (Mt)**	**2022 (Mt)**	**% 2023/2022**
	World	***1,888.2***	***1,888.7***	***0.0***
1	China	1,019.1	1,019.1	0.0
2	India	140.2	125.4	11.8
3	Japan	87.0	89.2	-2.5
4	United States	80.7	80.5	0.2
5	Russia (e)	75.8	71.7	5.6
6	South Korea	66.7	65.8	1.3
7	Germany	35.4	36.9	-3.9
8	Türkiye	33.7	35.1	-4.0
9	Brazil	31.9	34.1	-6.5
10	Iran	31.1	30.6	1.8
11	Italy	21.1	21.6	-2.4
12	Viet Nam (e)	19.0	20.0	-5.0
13	Taiwan, China (e)	18.9	20.8	-8.9
14	Mexico (e)	16.3	18.4	-11.6
15	Indonesia (e)	16.0	15.6	2.8
16	Canada (e)	12.3	12.1	1.3
17	Spain	11.3	11.6	-2.7
18	Egypt	10.4	9.8	5.4
19	France	10.0	12.1	-17.4
20	Saudi Arabia	9.9	9.9	0.8

Source : worldsteel.org


DASTUR
Green Steel
Flexible Design & Engineering
Environment & Sustainability
Techno-economic Assessments
Logistics & Distribution
Operations & Process Improvements
Advanced Analytics, Process Modeling, Simulation
Business
Technology
Engineering
Operations
India | Germany | USA | UAE | Japan
www.dastur.com
www.dasturenergy.com

Rs. 18/- (Notional) *RNI Regn No. 69992/98*